Stress/Damage Detection with Smart Concrete

Hua Liu and Aparna Deshmukh
Nathan Salowitz, Konstantin Sobolev and Jian Zhao
University of Wisconsin-Milwaukee
October 2023

IHM Plans – Bridge Structures

- Bridge structures
  - Bridge decks
  - Bridge girders
  - Expansion joints
  - Bearings
  - Bridge abutments
  - Bridge piers
  - Piles

- Data elements
  - Strains (internal and external)
  - Forces (internal and external)
  - Displacements
  - Vibrations
  - Cracking (loading and fatigue)
  - Corrosion
  - Chemical attack

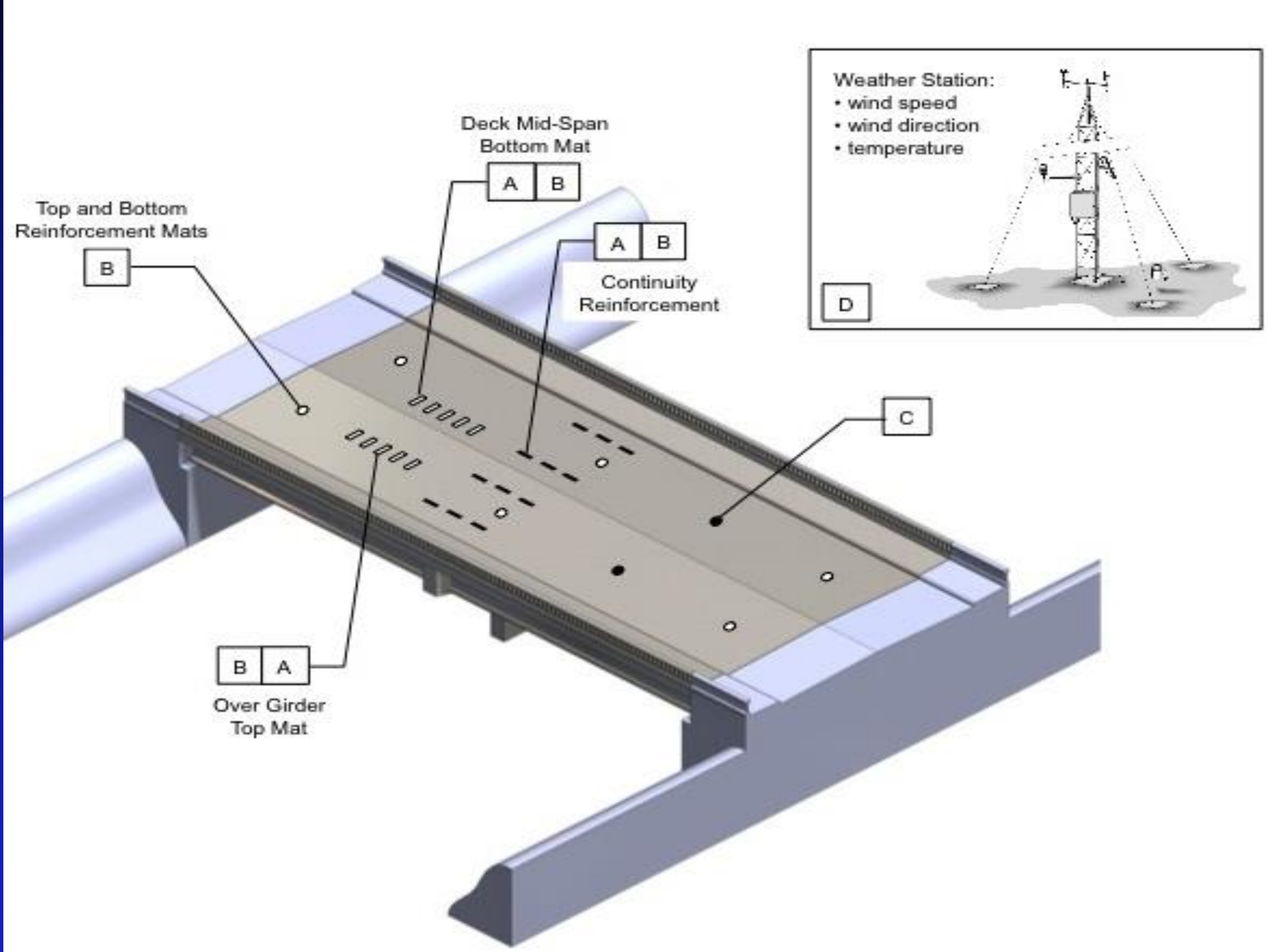

Smart Concrete - Portland Cement Mortar with Graphene Nano-Platelets (GnPs)

Mix Design	Specific Gravity	Weight (g/l)
Type 1 cement	3.15	975
Silica sand	2.6	975
Water	1.0	312
Megapol SP	1.19	1.95
GnPs	1.3	2.44
PVA fiber	1.15	11.5

Conductivity of Smart Concrete

- Contacting: direct contact of neighboring nanoscale fillers (GnPs), thus forming conductive links.
- Field emission: transmission conduction of electrons among the disconnected but close enough GnPs. Electrons jump through the energy barriers between GnPs in a cement-based matrix.
- Ionic conduction: motion of ions in pore solution, ionic conductivity varies in a particularly wide range when cement contains a substantial amount of free water.
- Bridging: GnPs connecting pores filled with conductive pore fluid

Conductivity of Smart Concrete under Loading

- Change of intrinsic resistance of nanoscale fillers.
- Change of bonding between functional filler and matrix.
- Change of contact between nanoscale fillers.
- Change of tunneling distance between nanoscale fillers.
- Change of capacitance

Han et al. (2012) stated that the capacitance of cement-based nanocomposites with carbon nanotubes is insensitive to an external force

Conductivity Measurements

Researchers have found some usable electrical signals to characterize the electromechanical behavior of cement-based nanocomposites, including electrical resistance or resistivity, electrical reactance, capacitance, relative dielectric constant, and electrical impedance tomography (EIT).

Research Objectives

- 4-probe AC with a Resipod (industry-standard method)
- Essentially EIT but with data processing
- Condition Detection: age, moisture, hydration, and stresses
- Damage detection - Currently only cracking with SC skin
- From R readings to back guess damage? Need machine learning
- Constitutive models for FE multi-physics analysis
- FE Analyses can predict the resistivity of beams and slabs
- Laboratory tests to verify FE analyses

Smart Concrete with GnPs – in Tension

- The prism was 38X12.7X160 mm
- The electrical resistance of the samples was measured using a Resipod surface resistivity meter for concrete from Proceq®
- 4-probe AC @ 40 Hz
- Plate electrodes were used with a resistor of 5 kilohm separating the current probes and potential probes
- A geometry factor (Kg) of 0.7313 to consider the impact of non-uniform current flow

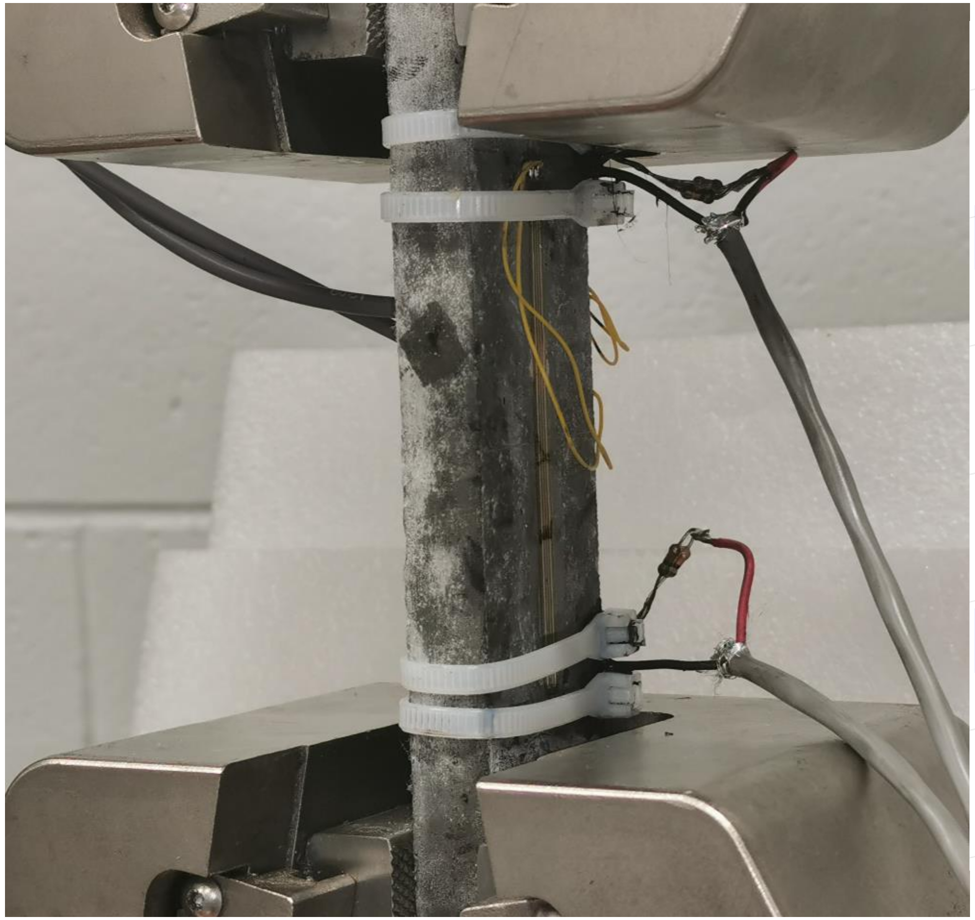

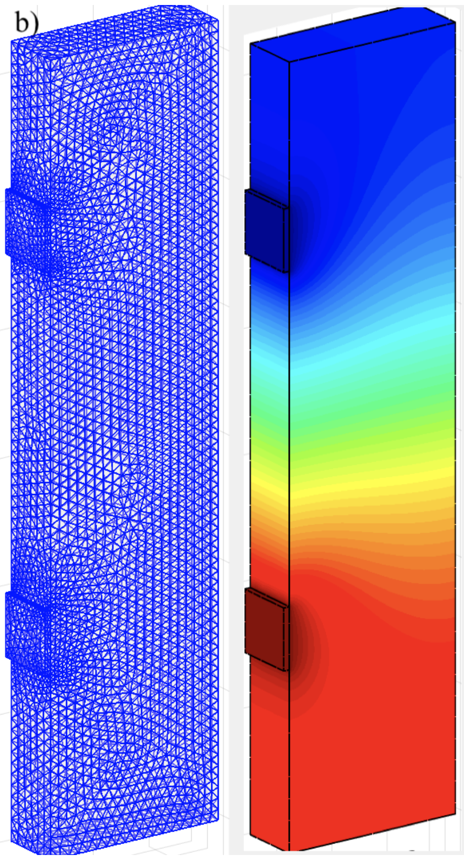

Smart Concrete with GnPs – in Tension

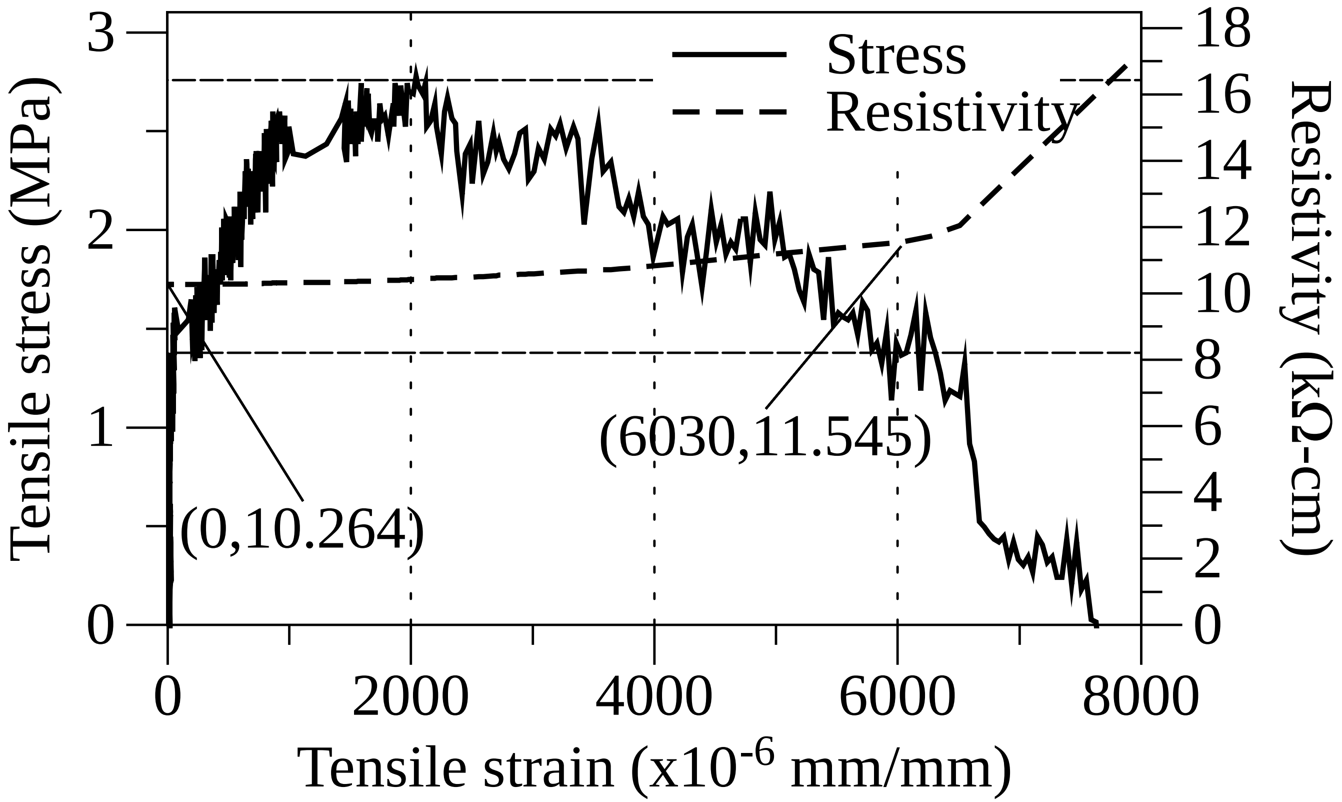

Smart Concrete with GnPs – in Tension

- The resistivity of the material (ρ) was 10.264 kΩ·cm when the strain was zero
- The resistivity of the material increased approximately linearly to 11.545 kΩ·cm when the tensile strain increased to 6,030 $\mu\varepsilon$.
- K_s is 20 kΩ·cm/mm/mm from a linear regression analysis.

$$\rho = \rho_0(1 + K_s\varepsilon)$$

Smart Concrete with GnPs – in Compression

- standard 50-mm cube specimen
- The electrical resistance of the samples was measured using a Resipod surface resistivity meter for concrete from Proceq®
- 4-probe AC @ 40 Hz
- Plate electrodes were used with a resistor of 5 kilohm separating the current probes and potential probes
- A geometry factor (Kg) of 1.0 as the electrodes covered the whole faces

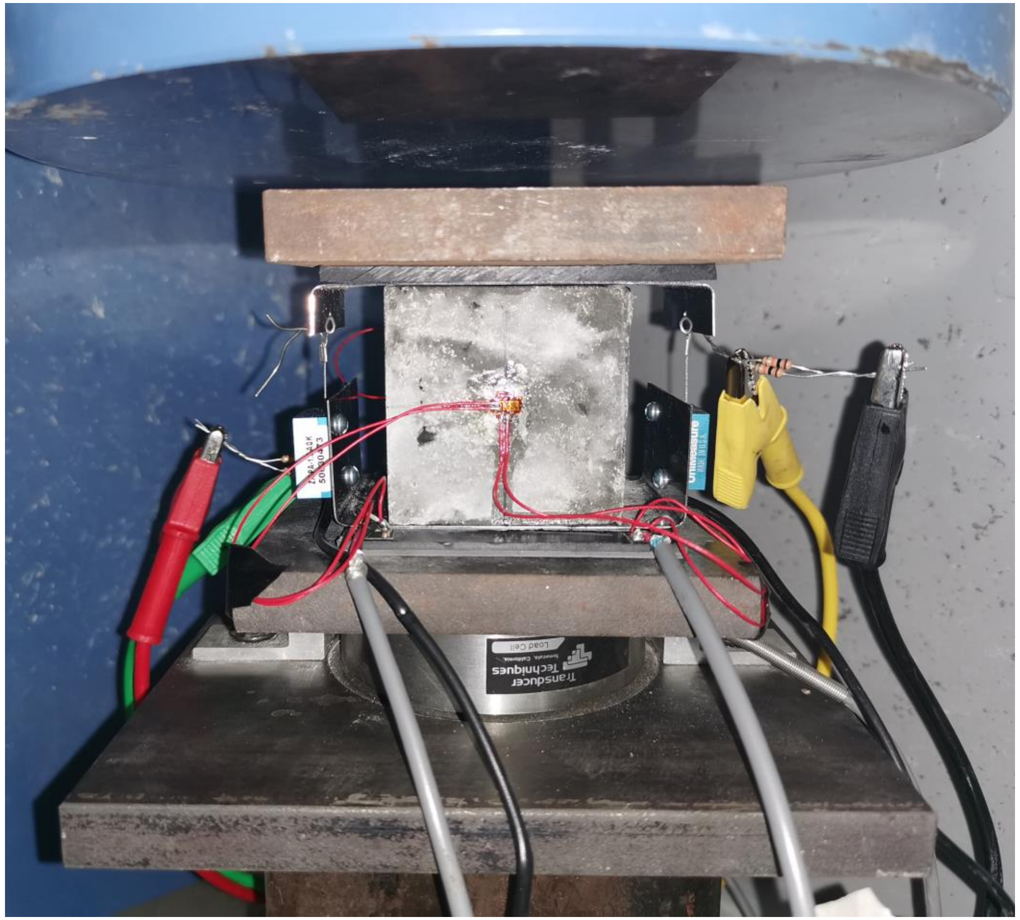

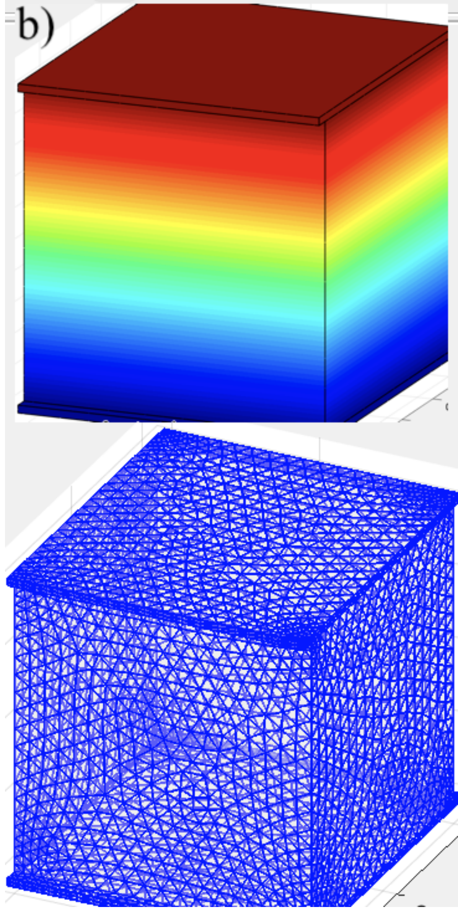

Smart Concrete with GnPs – in Compression

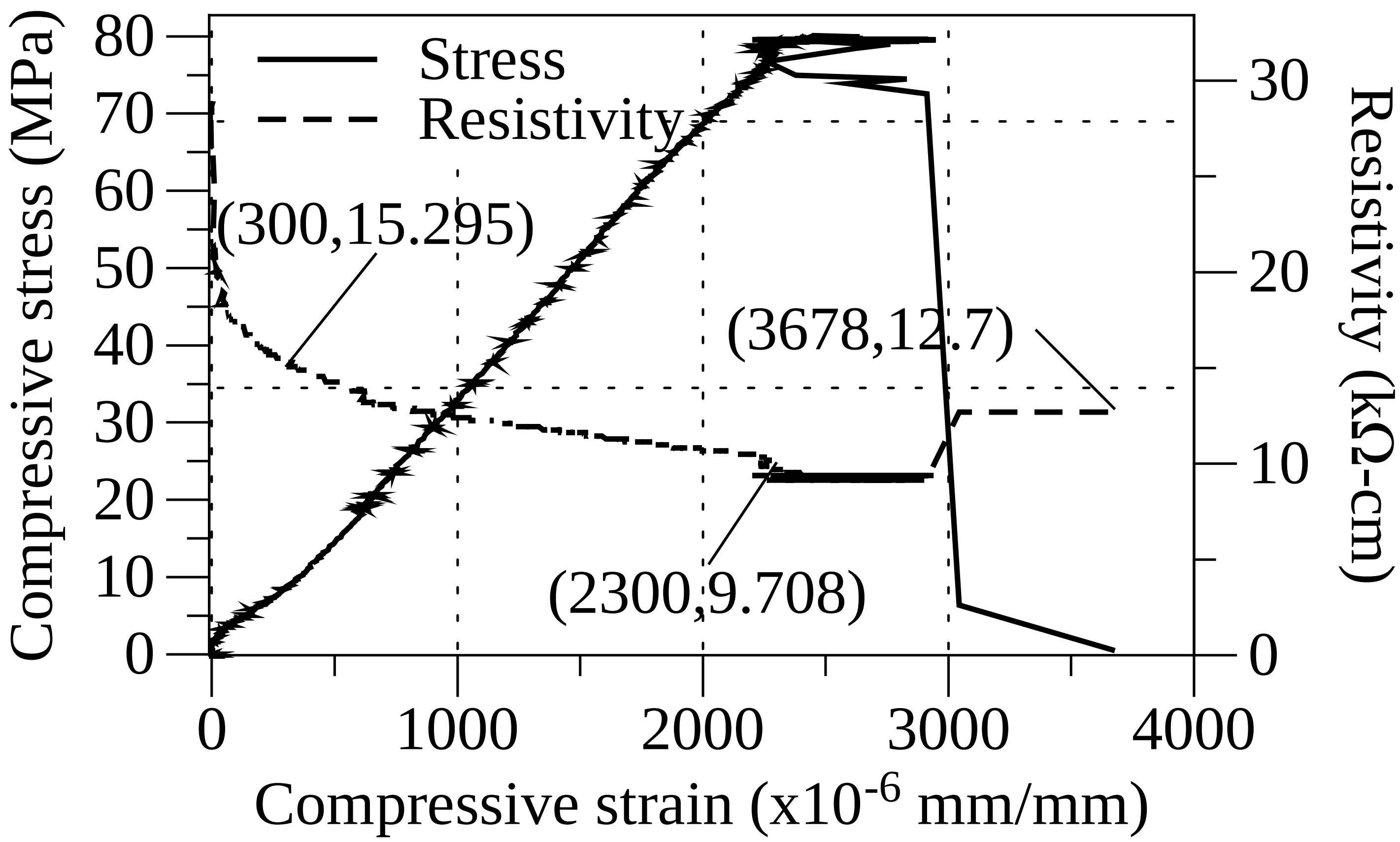

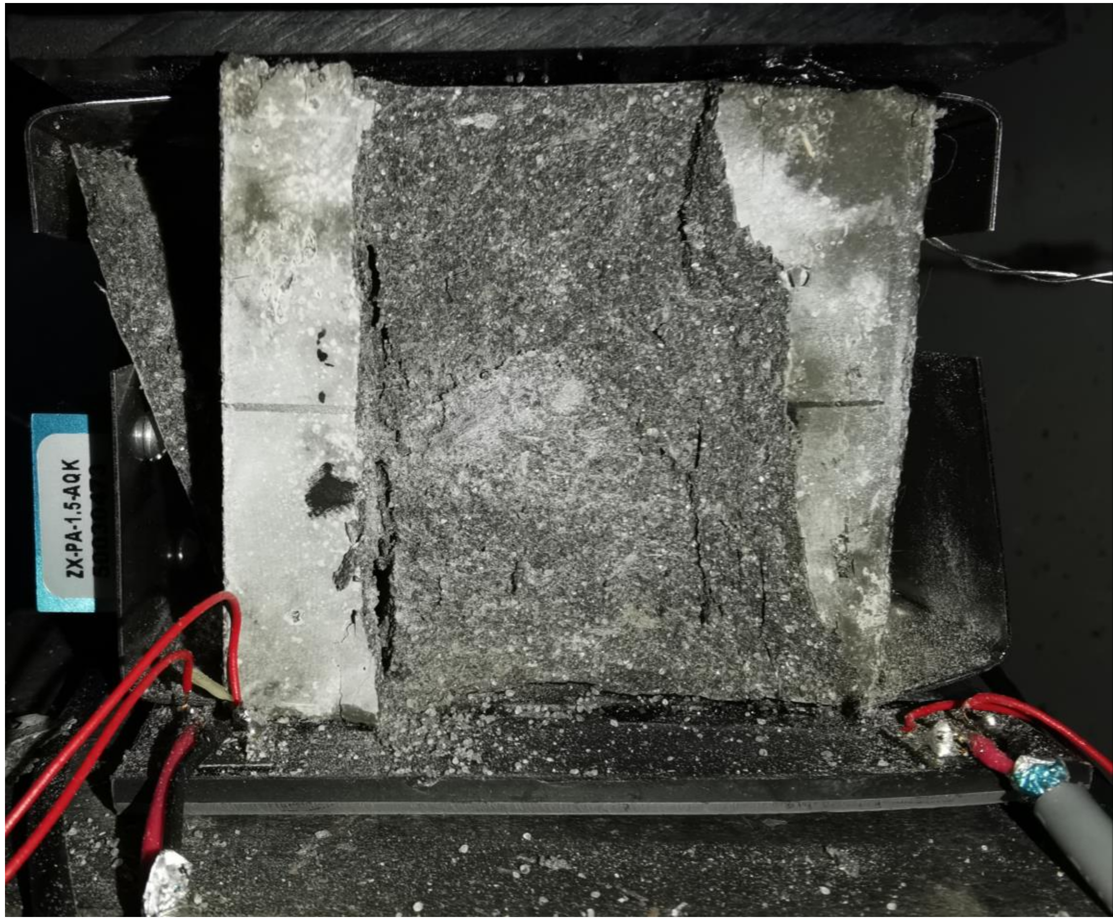

Smart Concrete with GnPs – in Compression

- The resistivity of the material (ρ) was 10.264 kΩ·cm when the strain was zero
- The resistivity of the material increased approximately linearly to 11.545 kΩ·cm when the tensile strain increased to 6,030 $\mu\varepsilon$.
- K_s is 200 kΩ·cm/mm/mm from a linear regression analysis.

$$\rho = \rho_0(1 + K_s \varepsilon)$$

Smart Concrete Slabs – Electrode Matrix

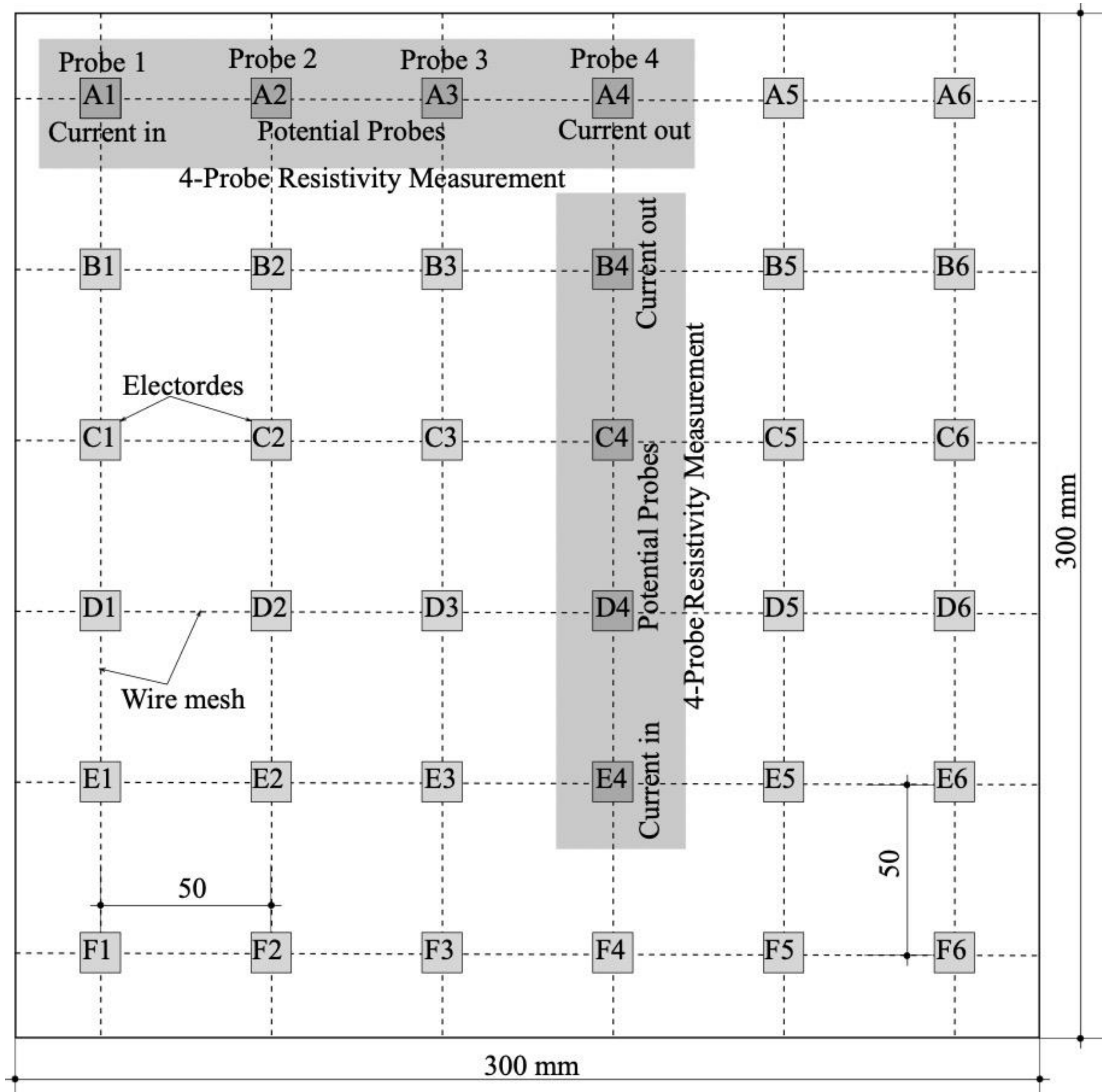

Smart Concrete Slabs – Resistivity Measurement

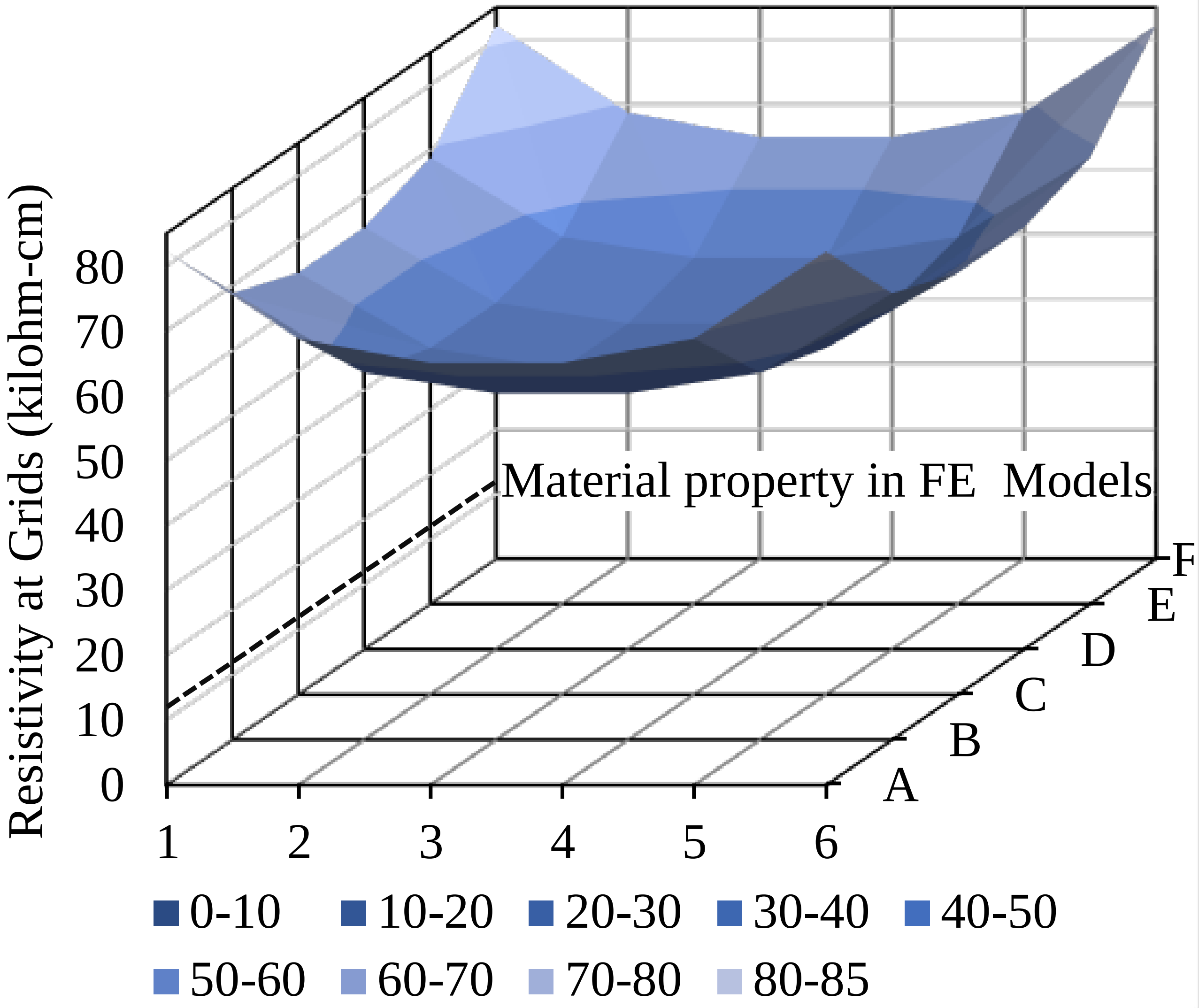

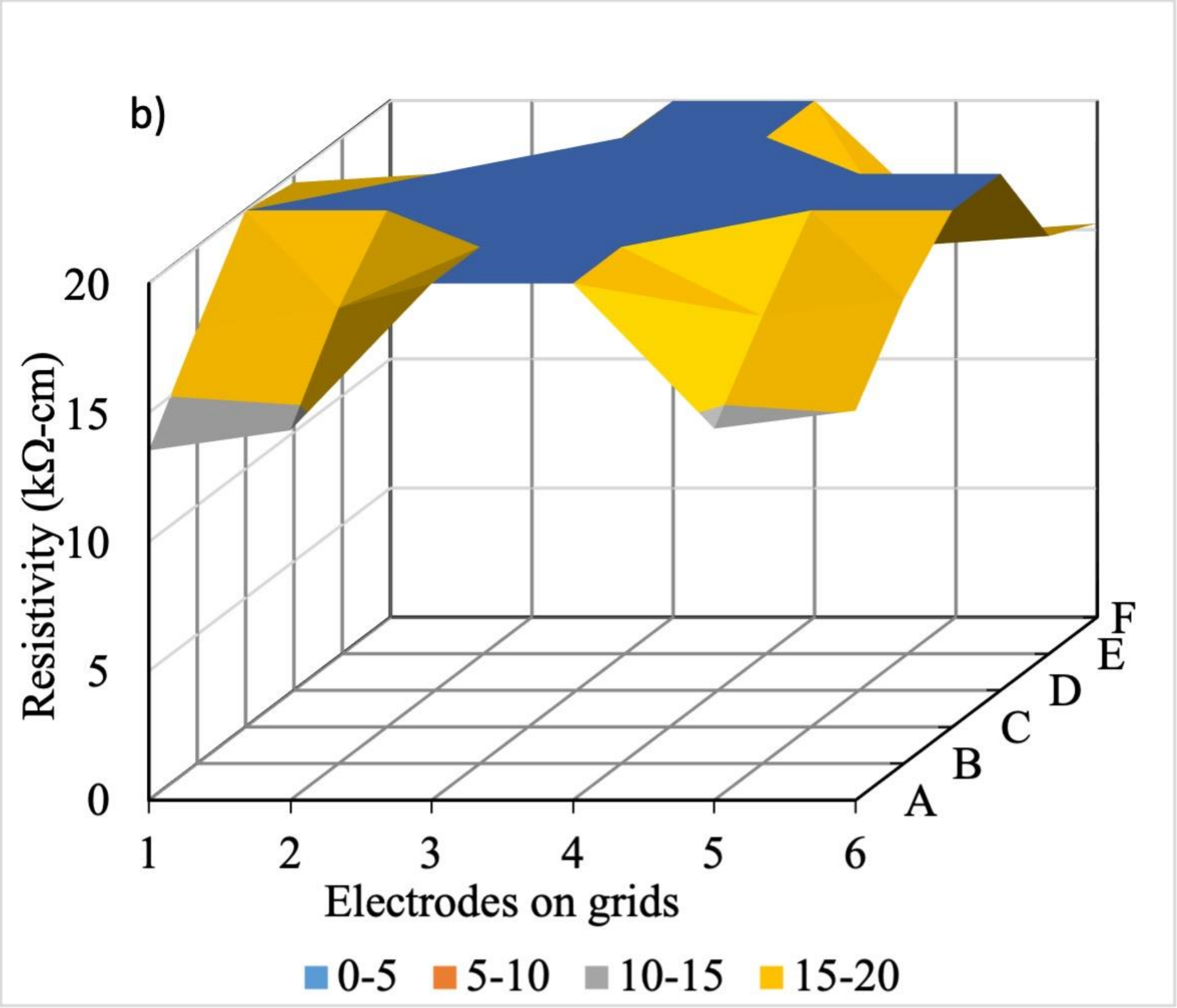

Smart Concrete Slabs – Geometry Corrections

$$K_w = \frac{1}{1+\frac{2}{\sqrt{1+\left(2\frac{l_w}{a}\right)^2}}-\frac{1}{\sqrt{1+\left(\frac{l_w}{a}\right)^2}}}.$$

Width Correction

$$K_l = \frac{1}{1+\frac{1}{2\frac{l_l}{a}+1}-\frac{1}{2\frac{l_l}{a}+2}-\frac{1}{2\frac{l_l}{a}+4}+\frac{1}{2\frac{l_l}{a}+5}}.$$

Length Correction

$$K_t = \frac{\left(\frac{t}{a}\right)^2+\frac{t}{a}}{\left(\frac{t}{a}\right)^2+0.75\frac{t}{a}+1.5}.$$

Thickness Correction

$$K_g = K_w K_l K_t. \qquad (5)$$

Total Correction

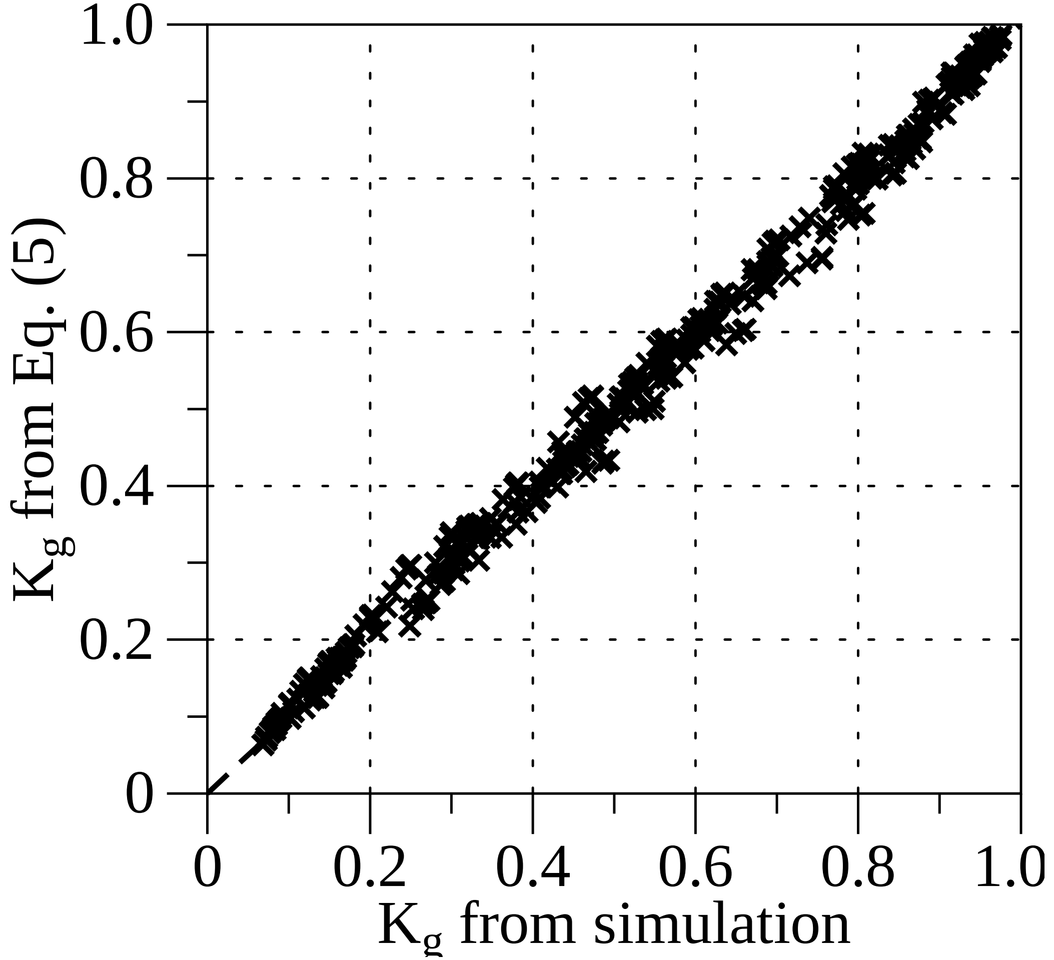

Smart Concrete Slabs – Laboratory Test

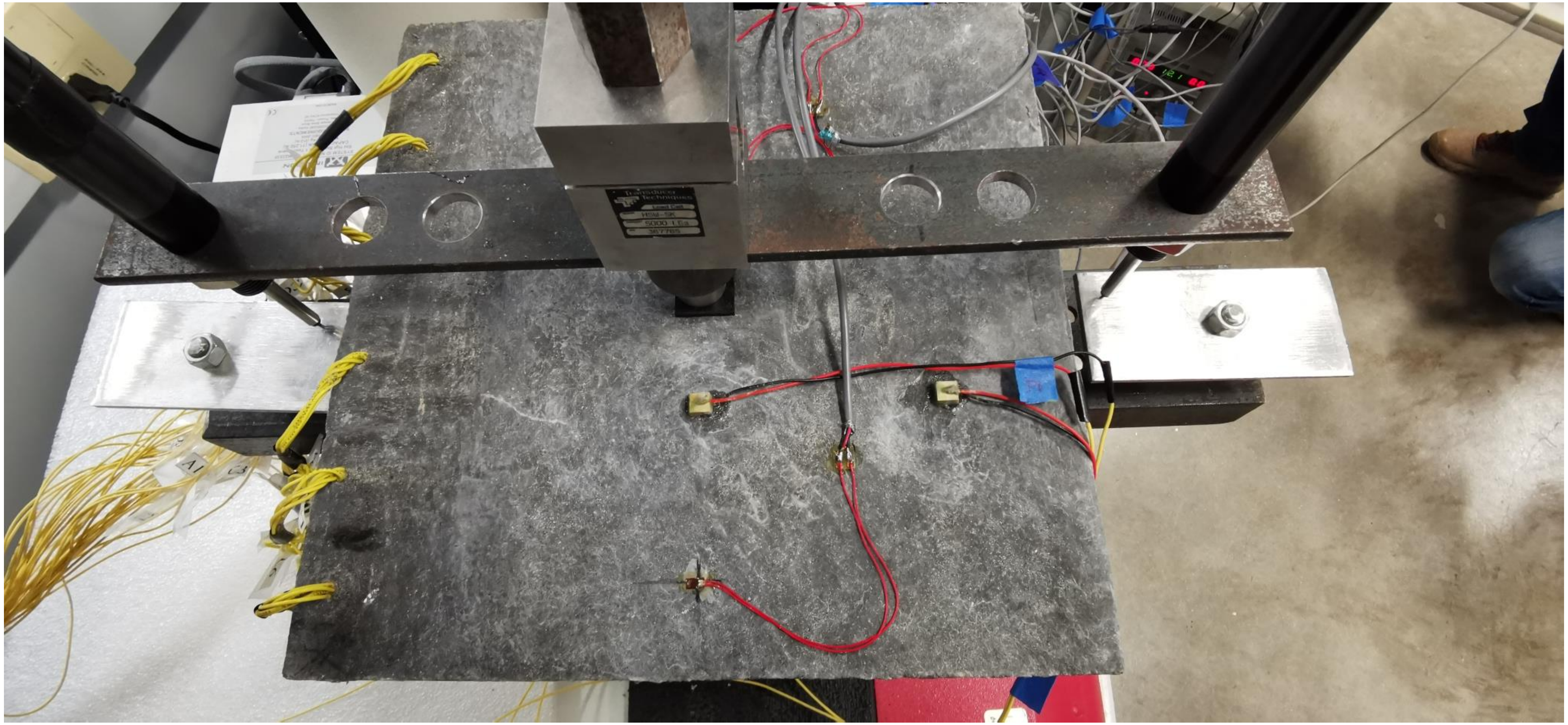

Smart Concrete Slabs – Finite Element Analysis

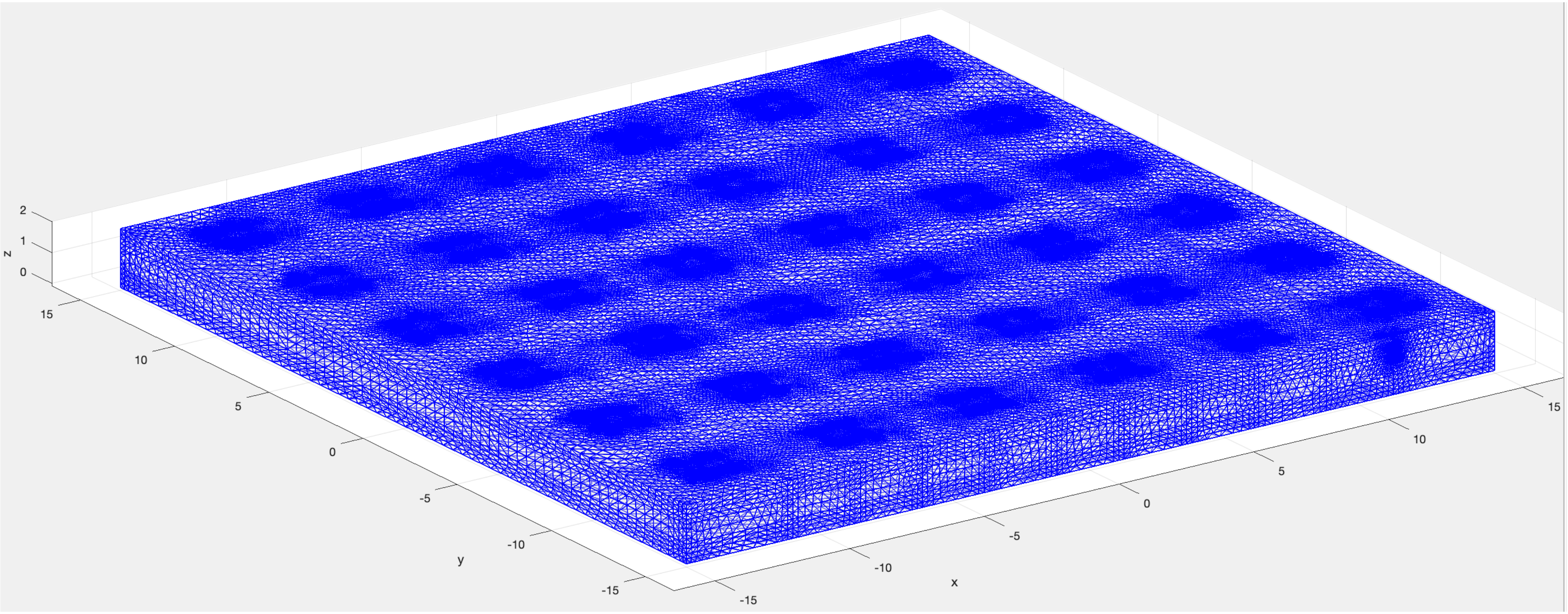

Smart Concrete Slabs – Simulated Stress Sensing

- Ks factor for materials in compression is 10 times that for materials in tension; therefore, upon loading the resistivity of slab should decrease
- This small change was clouded by the variations and two loose electrodes in measurements

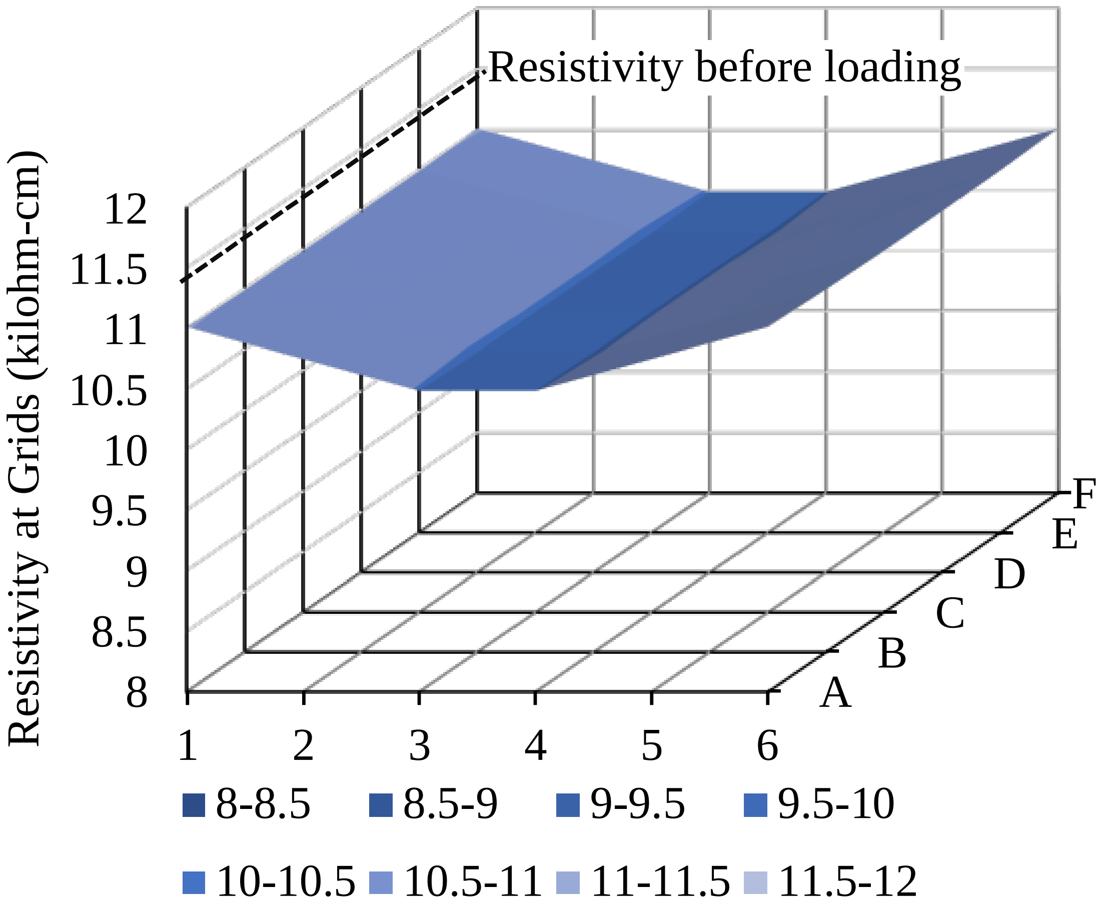

Smart Concrete Slabs – Damage Sensing

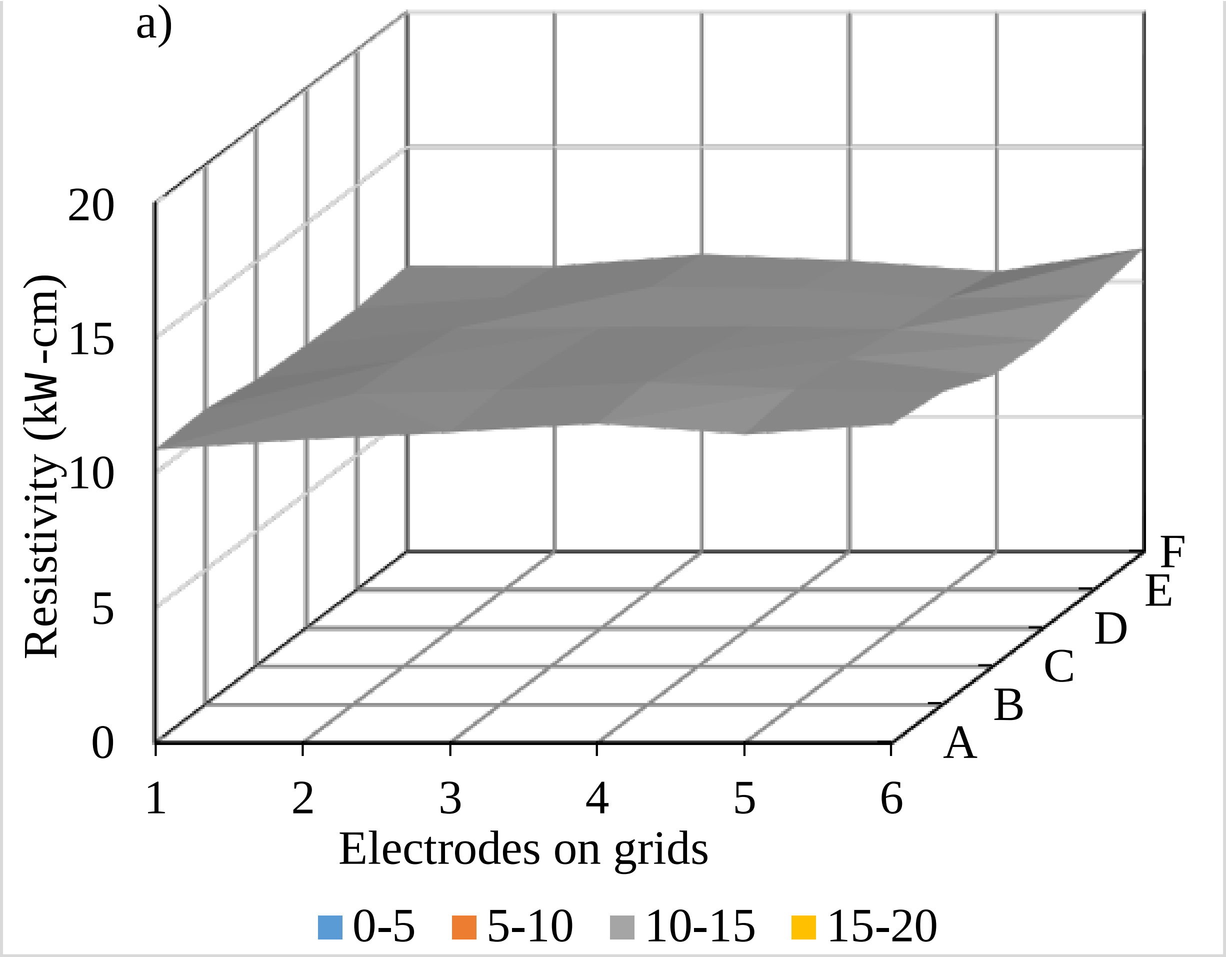

Before Loading

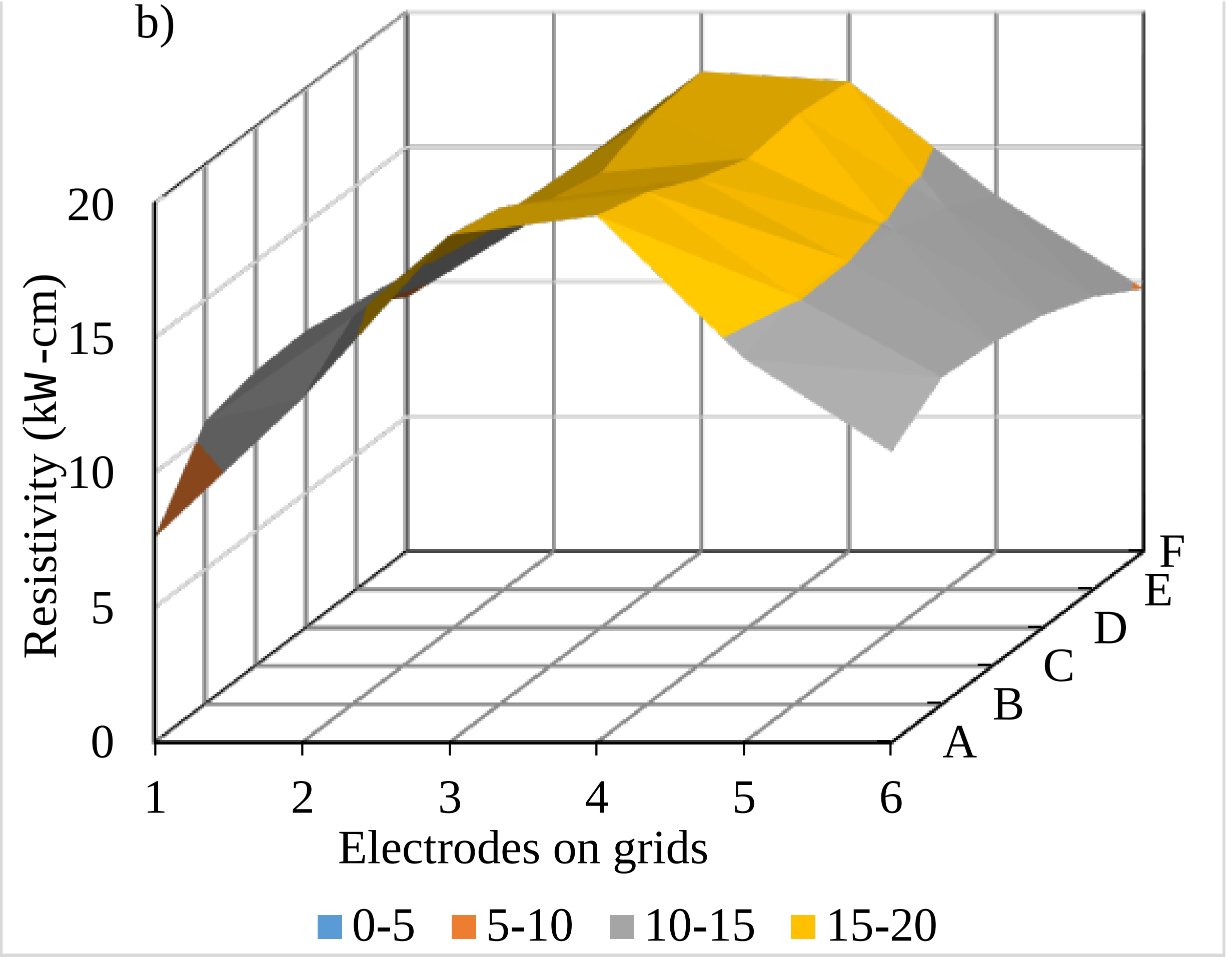

After Mid-Span Cracking

References

1915-Wenner A method for measuring earth resistivity
1954! Valdes Resistivity Measurements on Germanium for Transistors.pdf
1955-Uhlir The Potentials of Infinite Systems of Sources.pdf
1958-Smits Measurement of Sheet Resistivities using Four-Point Probe.pdf
1960-Hansen On the influence of shape and variations in conductivity of the sample on four-point measurements.pdf
1960-Hansen The influence of Shape on Four Point Measurement.pdf
1966-Haldor Topsoe_Geometric Factors in Four Point Resistivity Measurement.pdf
1996-Morris PRACTICAL EVALUATION OF RESISTIVITY OF CONCRETE.pdf
2000-Polder Test methods for on site measurement of resistivity of concrete.pdf
2001-Wen Uniaxial compression in carbon fiber reinforced cement sensed by electrical resistivity measurement in longitudinal and transverse directions.pdf
2004-Smith development-of-a-rapid-test-for-determining-the-transport-properties-of-concrete.pdf
2008-Newlands Sensitivity of electrode contact solutions and contact pressure in assessing electrical resistivity of concrete.pdf
2009-Hou Electrical Impedance Tomographic Methods for Sensing Strain Fields.pdf
2011_Han Nickel particle-based self-sensing pavement for vehicle detection.pdf
2011-Spragg Variability Analysis of the Bulk Resistivity Measured Using Concrete Cylinders.pdf
2012-Ardani Surface Resistivity Test Evaluation as an Indicator of the Chloride Permeability of Concrete.pdf
2013- Saafi Multifunctional properties of carbon nanotube/fly ash geopolymeric nanocomposites.pdf
2013-Peyvandi Enhancement of the durability characteristics of concrete using Graphene.pdf
2013-Spragg Factors That Influence Electrical Resistivity Measurements in Cementitious Systems.pdf
2014-Hallaji A new sensing skin for qualitative damage detection in concrete elements with electrical resistance tomography.pdf
2015-Layssi Electrical Resistivity of Concrete
2015-McCarter Two-point concrete resistivity measurements
2016-D'Alessandro Nanotube cement-matrix composites for SHM.pdf
2017_Chen Mechanical and smart properties of carbon fiber and graphite conductive concrete for internal damage monitoring of structure.pdf
2017_Erdem Self-sensing damage assessment and image-based surface crack quantification of carbon nanofibre reinforced concrete.pdf
2017-Azarsa Electrical Resistivity of Concrete for Durability Evaluation - A Review
2017! Downey Automated crack detection in conductive smart-concrete structures
2017-Konsta-Gdoutos Effect of CNT and CNF loading on conductivity and mechanical properties of nanomodified OPC mortars.pdf
2017-Proceq Resipod Family_Operating Instructions
2018-Aza Self Sensing Capability of Multifunctional Cementitious Nanocomposites.pdf
2018-Belli Evaluating the Self-Sensing Ability of Cement Mortars Manufactured with Graphene Nanoplatelets.pdf
2018-Du Mechanical Response and Strain Sensing of Cement Composites Added with Graphene Nanoplatelet under Tension.pdf
2018-Ge Piezoresistivity of Carbon Nanotube-Cement Composite.pdf
2018-Hambley Electrical Engineering book.pdf
2018-Meoni Strain Sensitivity of Smart Concrete Sensors Doped with Carbon Nanotubes
2018-Renvindran Effects of Graphene Nanoplatelet on the AC Electrical Conductivity of Epoxy Nanocomposites
2018-Wong Effects of Ultra-low Concentrations of Carbon Nanotubes on the Electromechanical Properties.pdf
2018-Wotring Characterizing the dispersion of graphene nanoplatelets in water with water reducing admixture.pdf
2019_Tian A state-of-the-art on self-sensing concrete Materials fabrication and properties.pdf
2019-Torgal Nanotechnology in eco-efficient construction materials (book)
2020-Cosoli Electrical Resistivity and Electrical Impedance Measurement in Mortar and Concrete Elements.pdf
2020-Cosoli Electrical Resistivity and Electrical Impedance Measurement.pdf
2020-DAlessandro Nanotechnology in cement-based construction (book).pdf

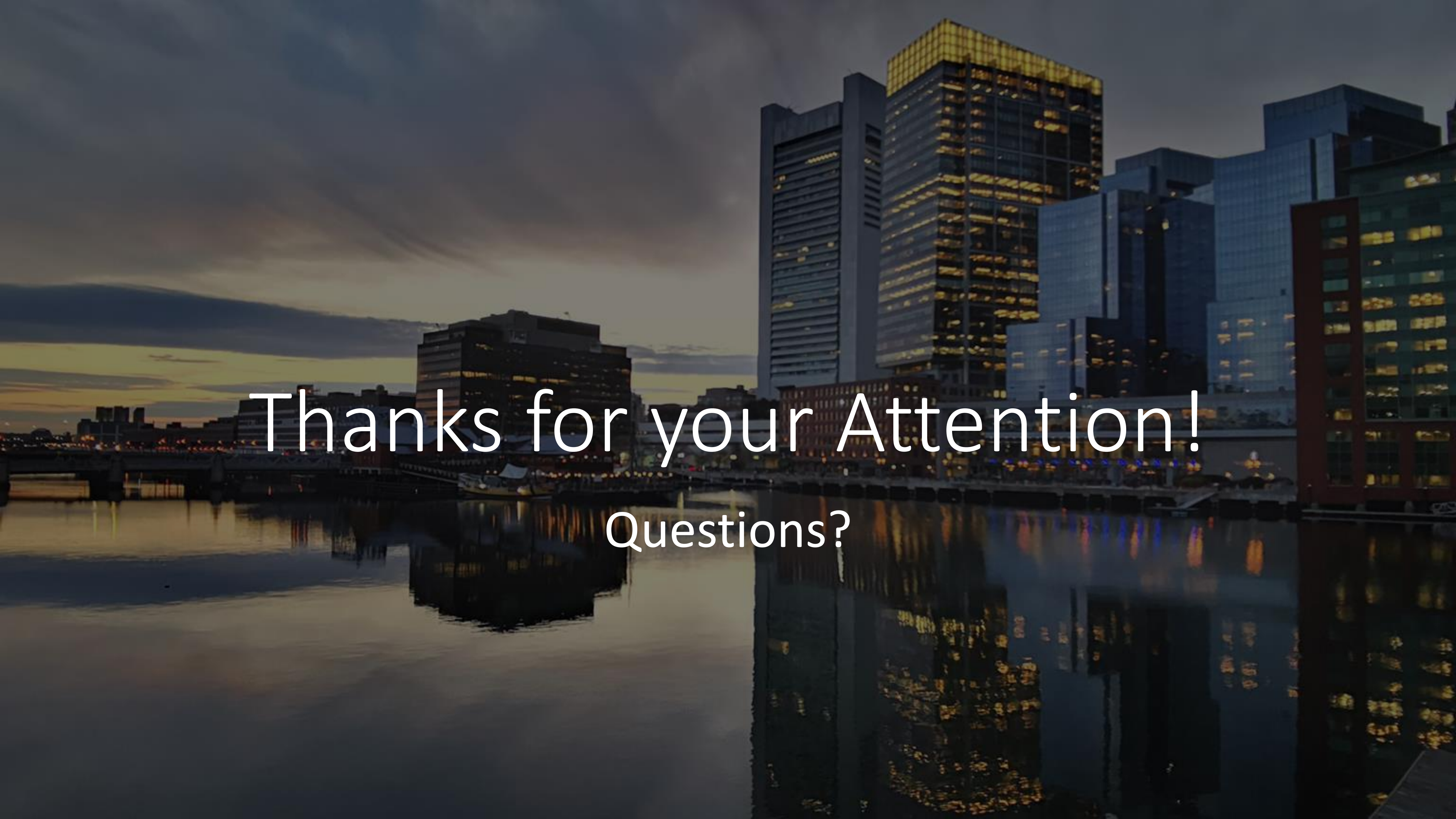

Thanks for your Attention!

Questions?

Existing Technologies on Smart Concrete Measurements:

2001 (Wen and Chung)

4-probe DC

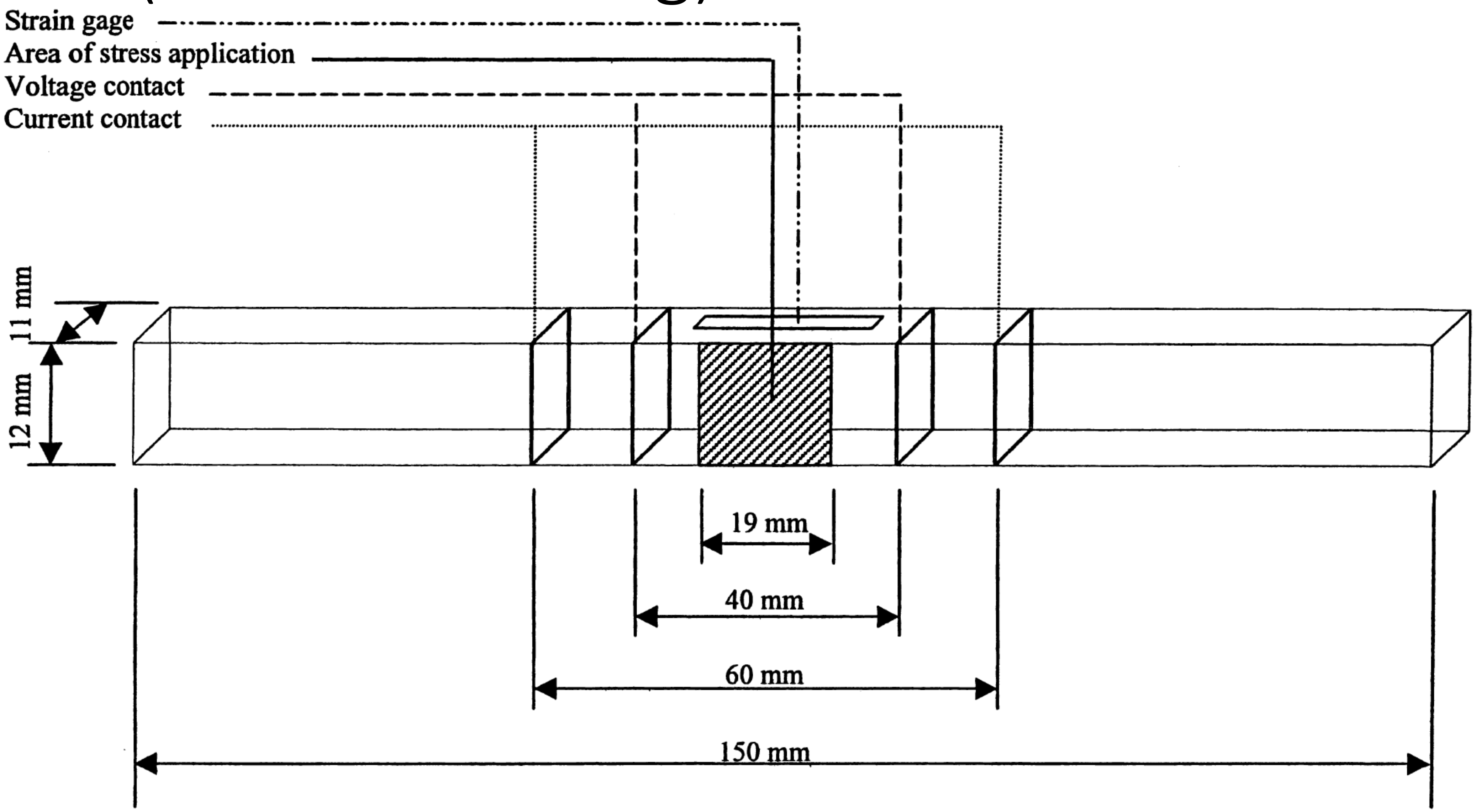

Fig. 1. Sample configuration for measuring the transverse electrical resistivity during uniaxial compression.

2009 (Hou and Lynch)

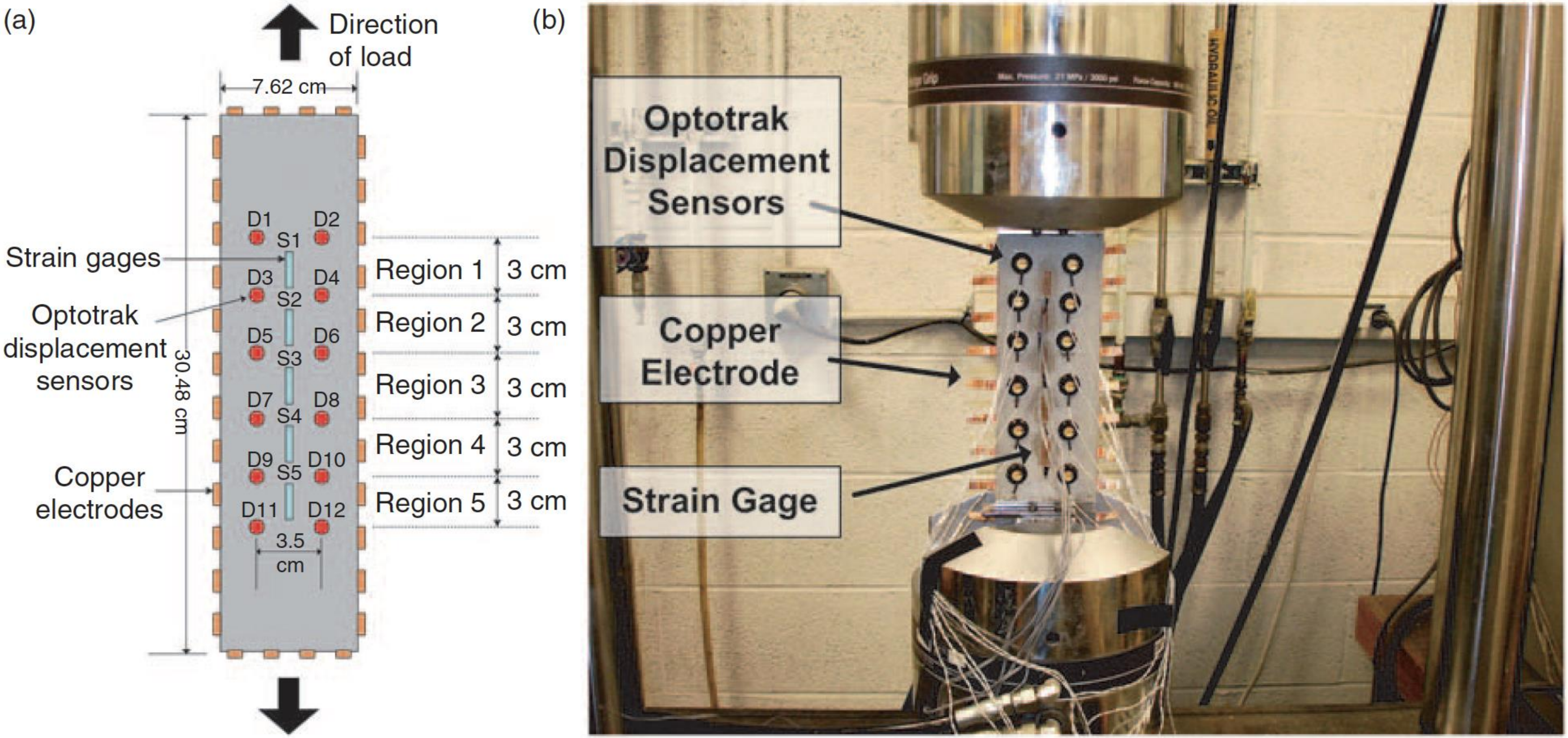

2009 (Hou and Lynch)

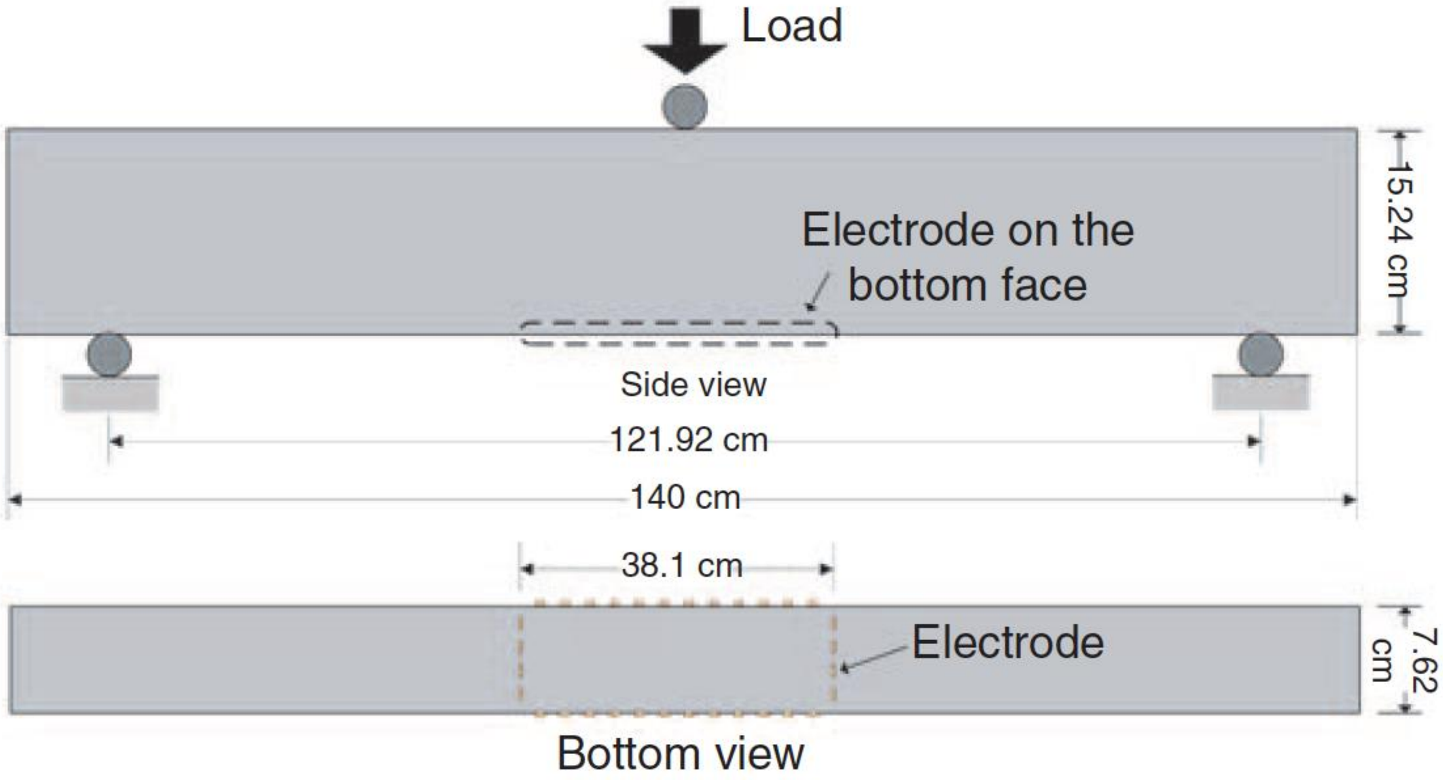

2012 (Hoheneder and Sobolev)

Composition	Reference FRC	CNF PVA-FRC
W/C	0.3	0.3
S/C	0.5	0.5
SP, % w cement	0.125	0.125
PVA fibers, % vol	3	3
Carbon nanofibers, %vol	0	0.2

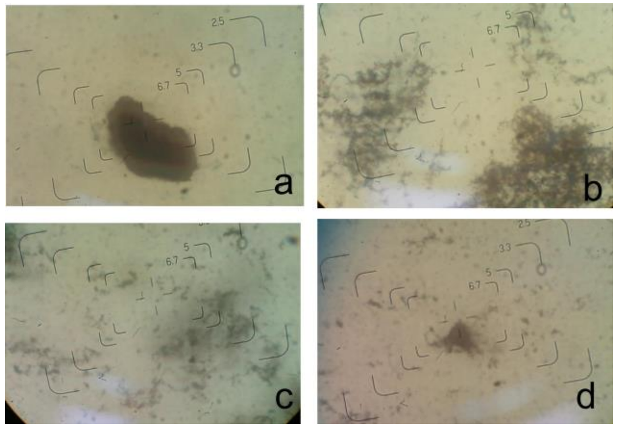

a) 5 min b) 10 min c) 15 min d) 20 min

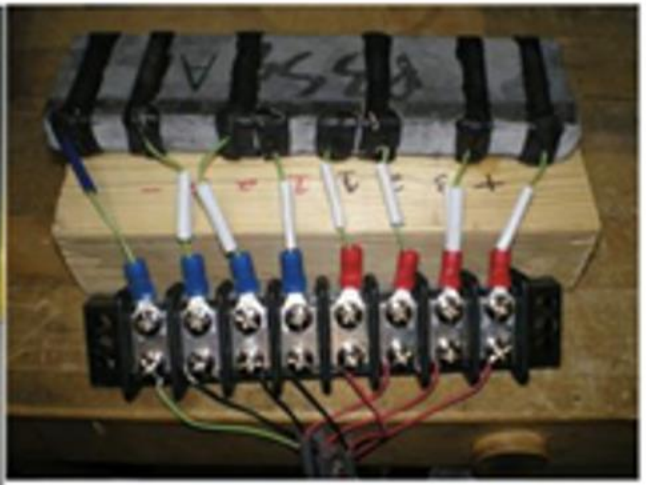

$$\Delta C / C_0 = \frac{C_t - C_0}{C_0}$$

2013 (Saafi et al.)

4-probe AC

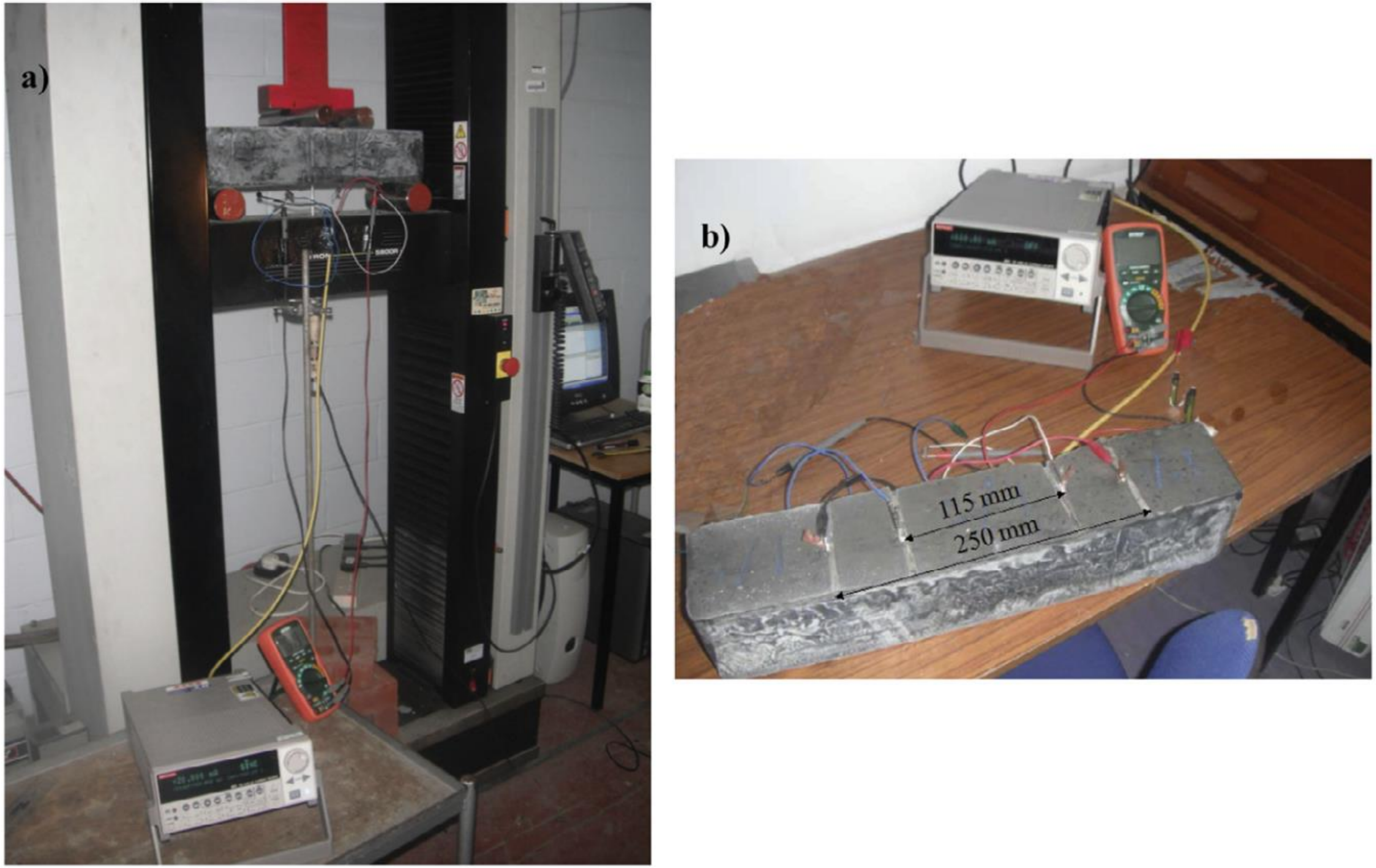

Fig. 4. Experimental setup. (a) Mechanical and piezoresistive characterization and (b) electrical characterization.

2014 (Halaji) EIT: Electrical Impedance Tomography

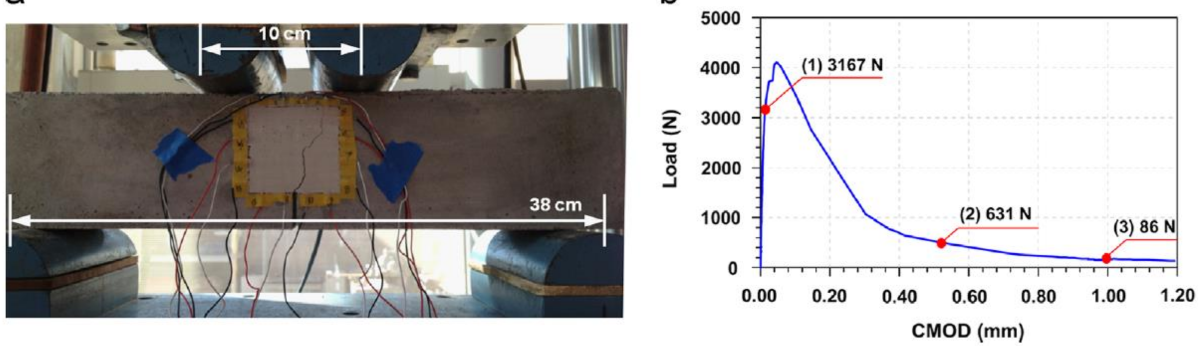

Fig. 6. (a) Photograph of the notched beam, (b) load versus Crack Mouth Opening Displacement (CMOD) curve of the notched beam.

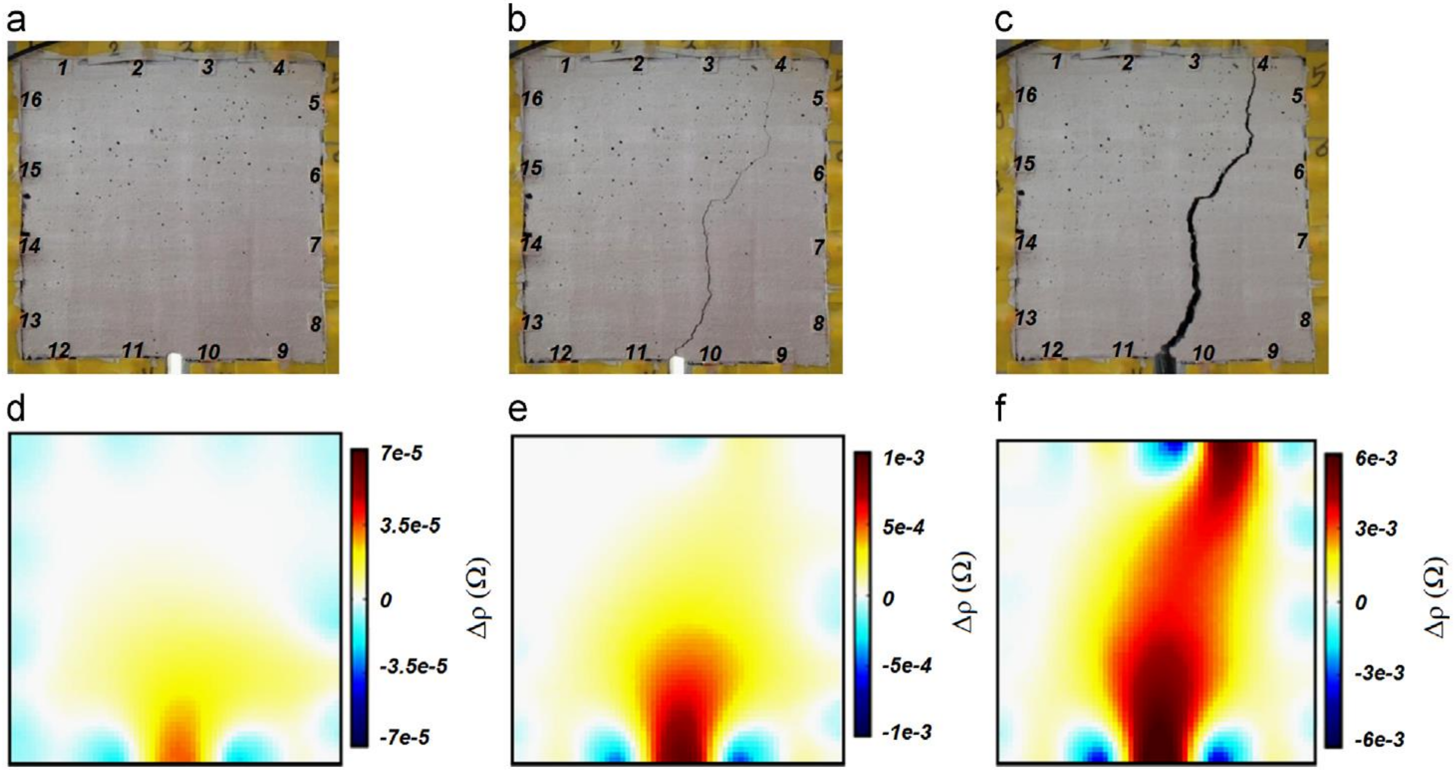

'ig. 7. (a)–(c) Photograph of the sensing skin at three different load levels shown in Fig. 6b, (d)–(f) ERT images of sensing skins at three different load levels shown i

2016 (D'Alessandro et al.)

4-probe DC and AC

A. D'Alessandro et al. / Cement and Concrete Composites 65 (2016) 200–213

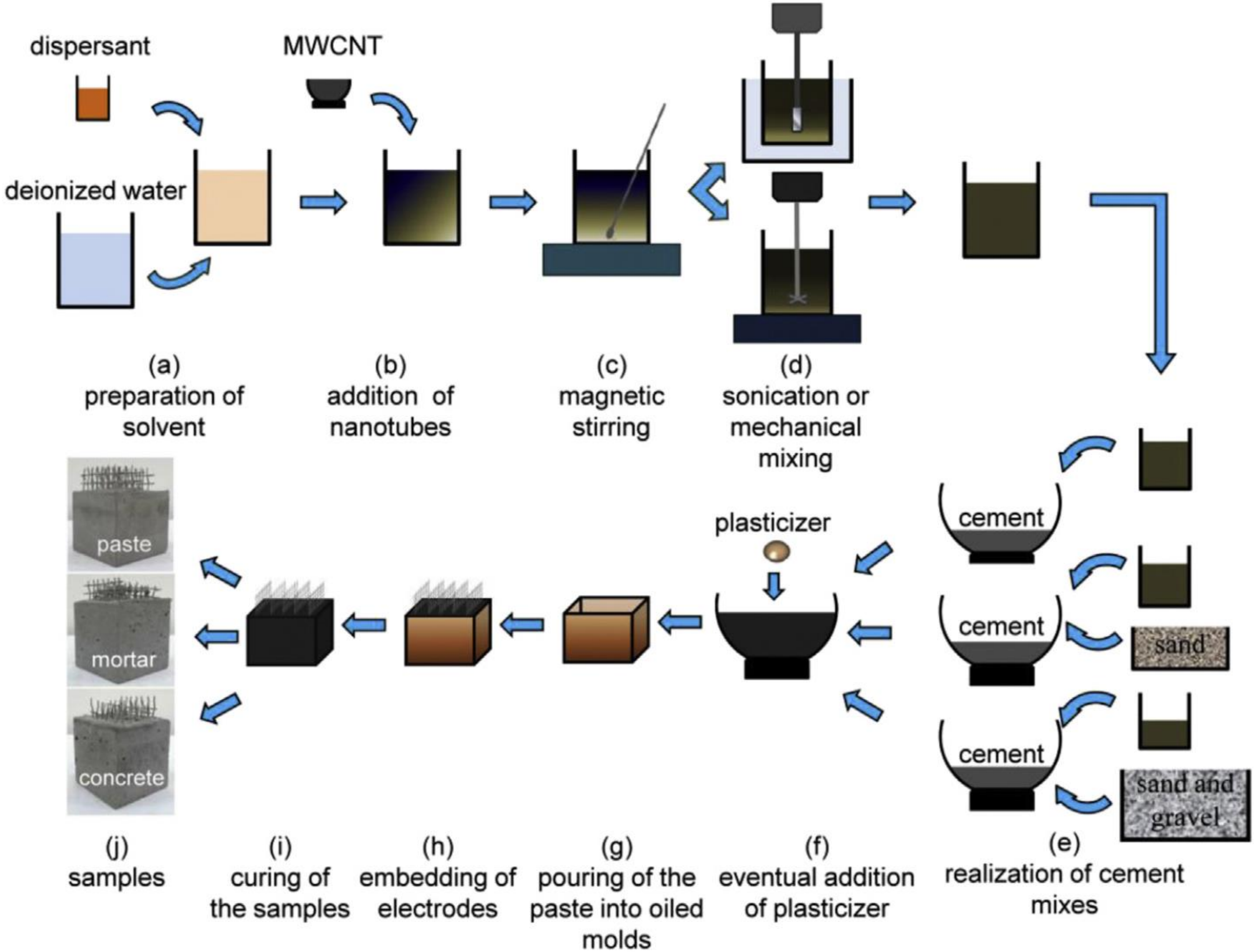

2016 (D'Alessandro et al.)

4-probe DC and AC

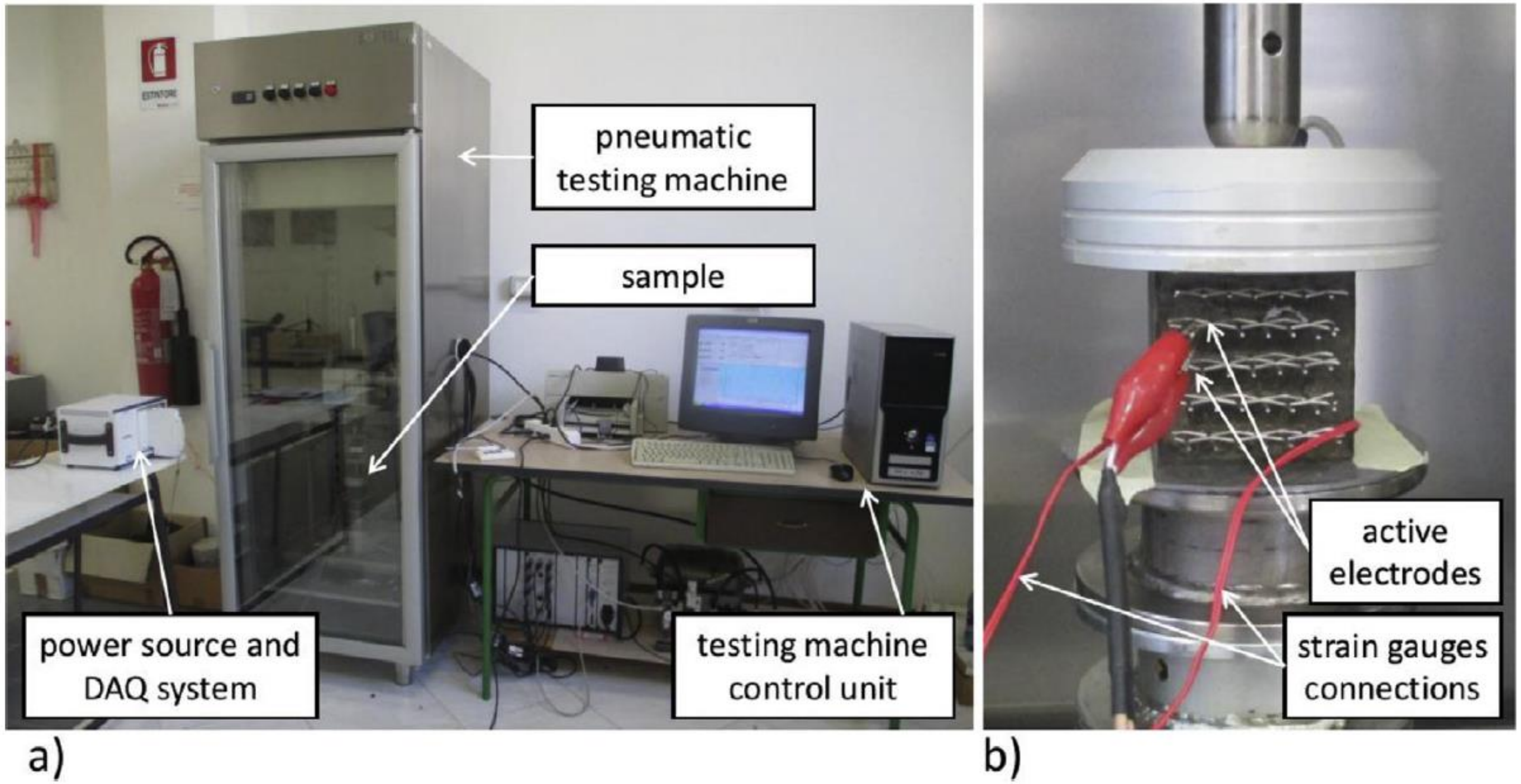

Fig. 5. a) Test set-up for strain sensing assessment of the composite materials; b) detailed view of coaxial cables connected to the net electrodes of the sample.

2016 (Gupta et al.)

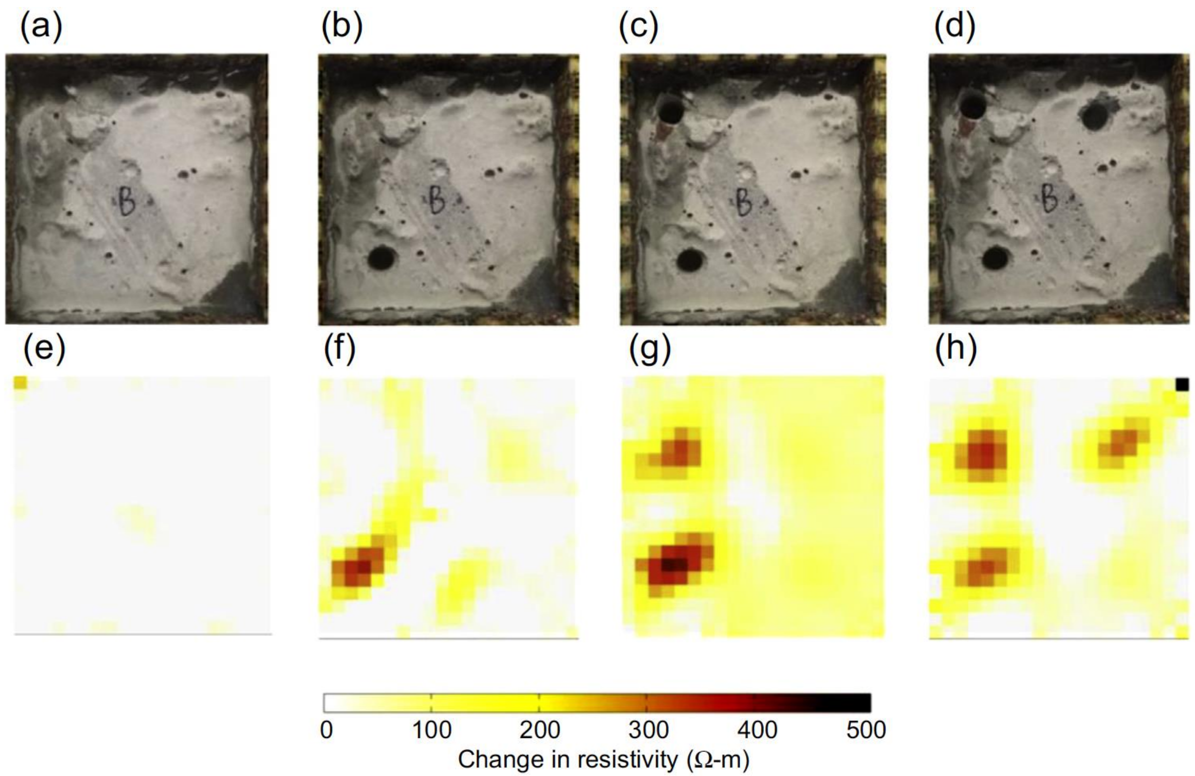

Figure 11.5 Damage detection tests were performed on the concrete plates cast using large aggregates coated with MWCNT-latex thin films (Gupta et al., 2016).

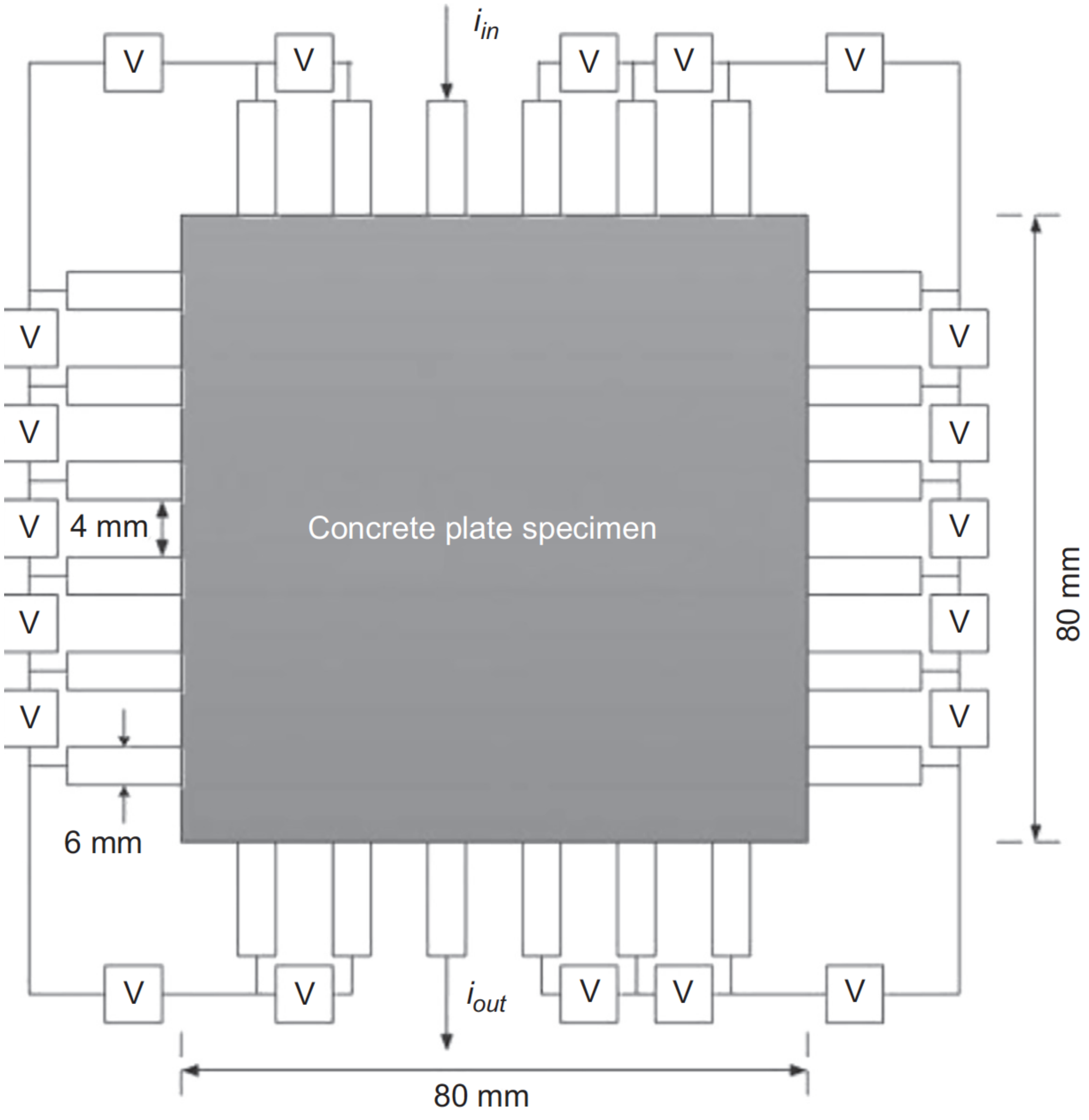

igure 11.4 Schematic of an EIT system (Gupta et al., 2016).

2018 (Meoni et al.)

4-probe DC

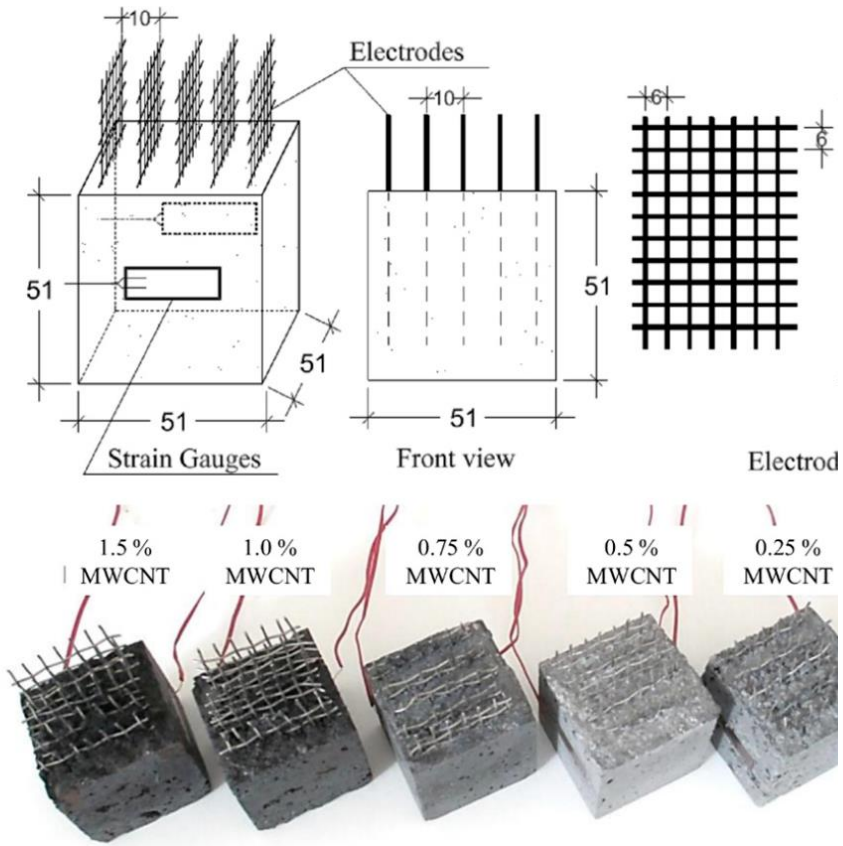

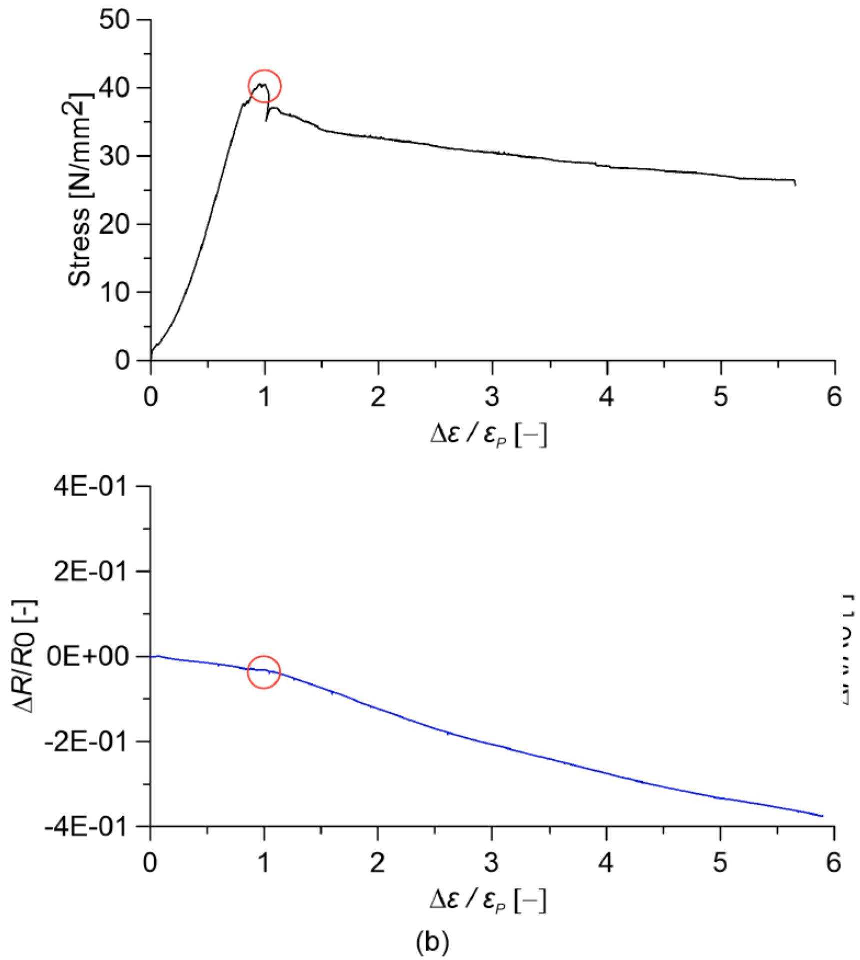

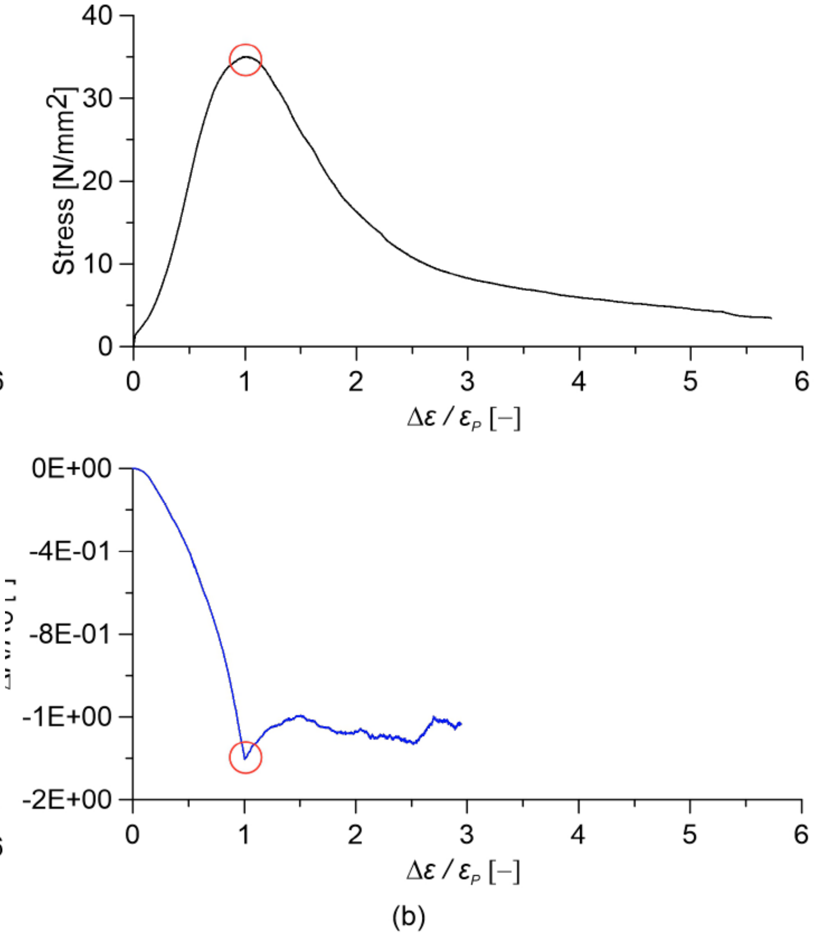

tive change in electrical resistance versus rel
axial destructive tests (the circle indicates the
s and (**b**) 0.50% MWCNTs.

e change in electrical resistance versus re
m destructive tests (the circle indicates the
l (**b**) 1.00% MWCNTs.

2018 (Aza)

4-Probe DC

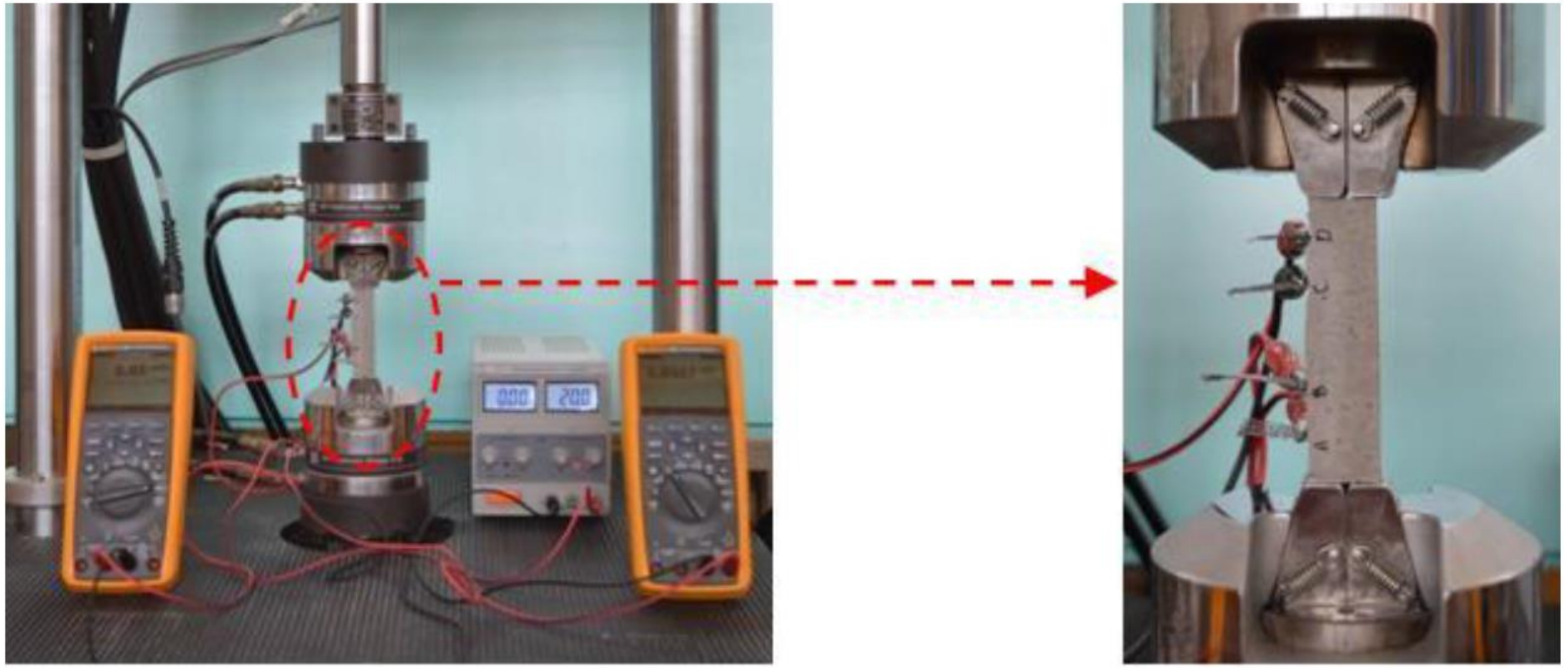

Fig. 1. Experimental setup for measuring the electrical resistance under compressive load

2020 (Laflamme and Ubertinib) 2-Probe AC, LCR meter @ 100k Hz

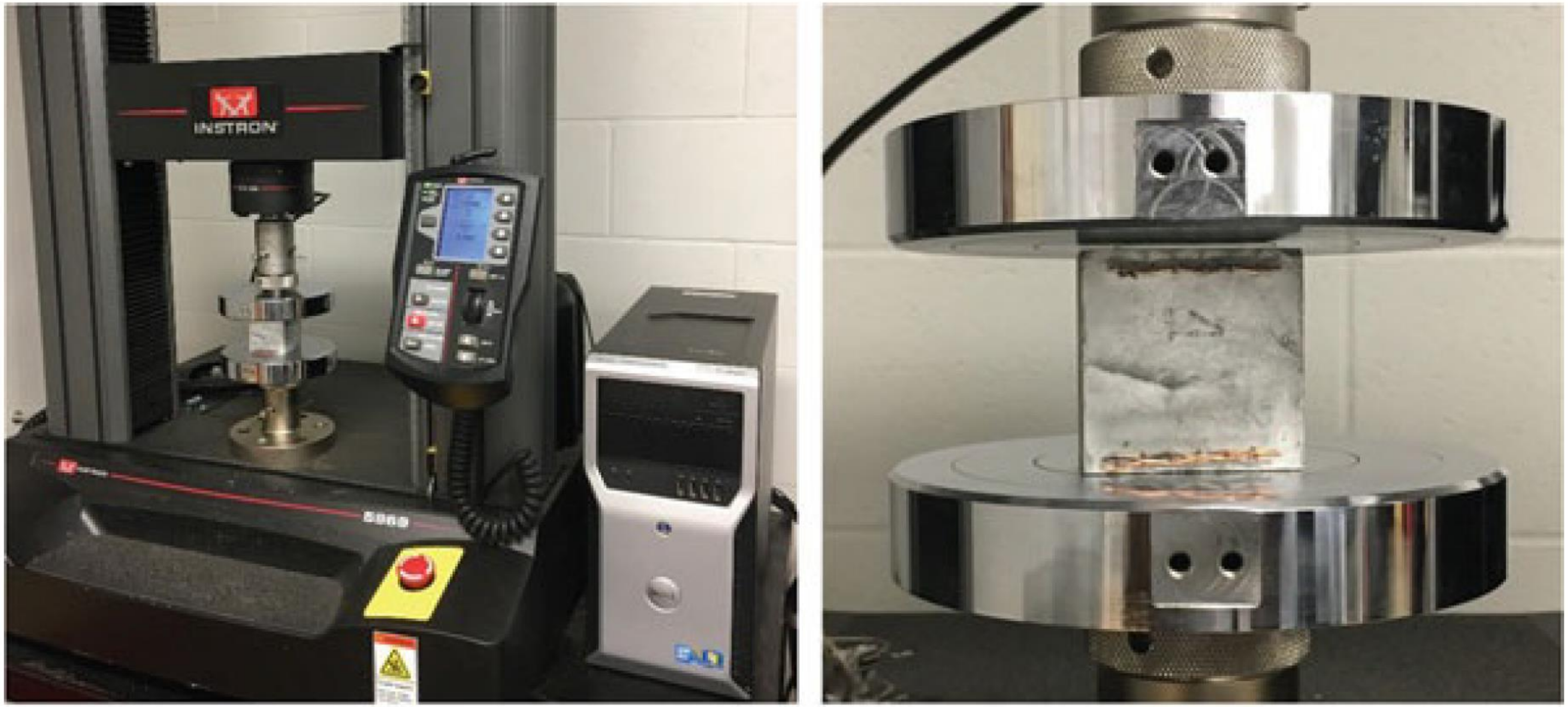

(a) (b)

Figure 3.5 Experimental configuration. (a) Cementitious sensor installed in the universal testing machine and

What are we trying to achieve?

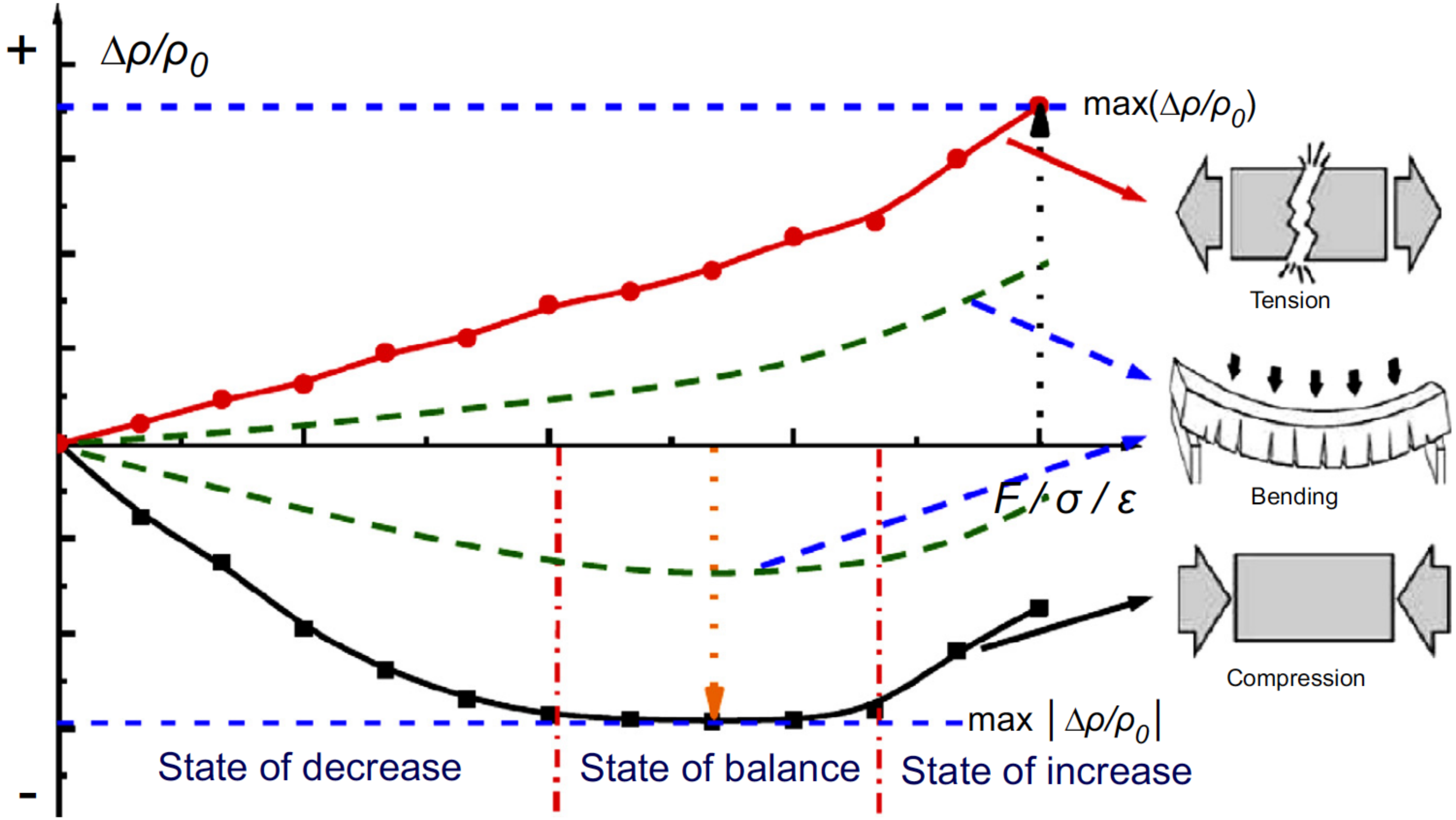

Figure 11.8 Typical sensing behavior of ISSC under loading (Han et al., 2015d).